Cell

Whitefly hijacks a plant detoxification gene that neutralizes plant toxins

Graphical abstract

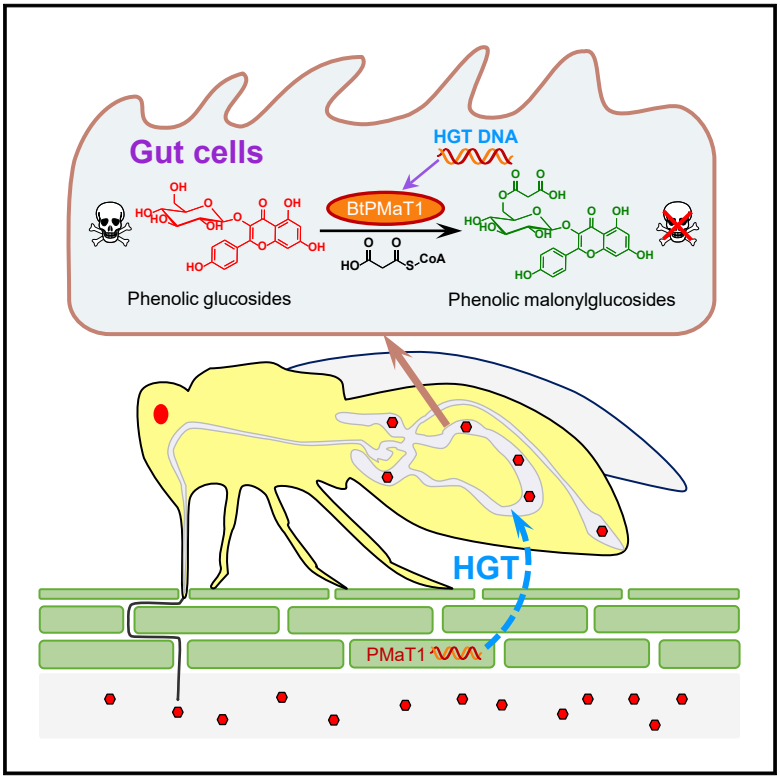

Highlights

- Many plants contain phenolic glycosides that are toxic for insect herbivores
- Whitefly carries a plant-derived phenolic glucoside malonyltransferase gene *BtPMaT1*
- *BtPMaT1* enables whiteflies to neutralize phenolic glycosides in host plants
- Plant-mediated silencing of *BtPMaT1* confers tomato full resistance to whiteflies

Authors

Jixing Xia, Zhaojiang Guo, Zezhong Yang, ..., Wannes Dermauw, Ted C.J. Turlings, Youjun Zhang

Correspondence

ted.turlings@unine.ch (T.C.J.T.), zhangyoujun@caas.cn (Y.Z.)

In brief

The cosmopolitan agricultural pest *Bemisia tabaci* has acquired a plant-derived gene through a plant-to-insect horizontal gene transfer event. This acquired gene allows whiteflies to detoxify plant defense compounds and continue to feed on their plant hosts.

Xia et al., 2021, Cell *184*, 1693–1705
April 1, 2021
https://doi.org/10.1016/j.cell.2021.02.014

CellPress

Cell

CellPress

Article

Whitefly hijacks a plant detoxification gene that neutralizes plant toxins

Jixing Xia,[1,7] Zhaojiang Guo,[1,7] Zezhong Yang,[1,7] Haolin Han,[1] Shaoli Wang,[1] Haifeng Xu,[1] Xin Yang,[1] Fengshan Yang,[2] Qingjun Wu,[1] Wen Xie,[1] Xuguo Zhou,[3] Wannes Dermauw,[4,5] Ted C.J. Turlings,[6,*] and Youjun Zhang[1,8,*]

[1]Department of Plant Protection, Institute of Vegetables and Flowers, Chinese Academy of Agricultural Sciences, Beijing 100081, China
[2]Key Laboratory of Molecular Biology of Heilongjiang Province, College of Life Sciences, Heilongjiang University, Harbin 150080, China
[3]Department of Entomology, University of Kentucky, Lexington, KY 40546-0091, USA
[4]Flanders Research Institute for Agriculture, Fisheries and Food (ILVO), Plant Sciences Unit, 8920 Merelbeke, Belgium
[5]Department of Plants and Crops, Faculty of Bioscience Engineering, Ghent University, Coupure Links 653, 9000 Ghent, Belgium
[6]Laboratory of Fundamental and Applied Research in Chemical Ecology, Institute of Biology, University of Neuchâtel, 2000 Neuchâtel, Switzerland
[7]These authors contributed equally
[8]Lead contact
*Correspondence: ted.turlings@unine.ch (T.C.J.T.), zhangyoujun@caas.cn (Y.Z.)
https://doi.org/10.1016/j.cell.2021.02.014

SUMMARY

Plants protect themselves with a vast array of toxic secondary metabolites, yet most plants serve as food for insects. The evolutionary processes that allow herbivorous insects to resist plant defenses remain largely unknown. The whitefly *Bemisia tabaci* is a cosmopolitan, highly polyphagous agricultural pest that vectors several serious plant pathogenic viruses and is an excellent model to probe the molecular mechanisms involved in overcoming plant defenses. Here, we show that, through an exceptional horizontal gene transfer event, the whitefly has acquired the plant-derived phenolic glucoside malonyltransferase gene *BtPMaT1*. This gene enables whiteflies to neutralize phenolic glucosides. This was confirmed by genetically transforming tomato plants to produce small interfering RNAs that silence *BtPMaT1*, thus impairing the whiteflies' detoxification ability. These findings reveal an evolutionary scenario whereby herbivores harness the genetic toolkit of their host plants to develop resistance to plant defenses and how this can be exploited for crop protection.

INTRODUCTION

During more than 400 million years of co-evolution with insect herbivores (Price et al., 2011), plants have developed a highly diverse spectrum of morphological (Higuchi and Kawakita, 2019), molecular (Erb and Reymond, 2019), and biochemical (Mithöfer and Boland, 2012) defenses to withstand insect attack. Among the biochemical defenses, plant secondary metabolites are the most diverse and effective weapons that can be attributed to herbivore-plant co-evolution (Speed et al., 2015).

Phenolic glycosides, which are comprised of a sugar unit bound to a phenol aglycone, are among the most abundant plant secondary metabolites. They strongly affect growth, development, and behavior of insect herbivores (Boeckler et al., 2011; Leiss et al., 2009; Mierziak et al., 2014; Onkokesung et al., 2014). In plants, an important modification of phenolic glycosides involves their malonylation, which is regulated by phenolic glucoside malonyltransferases (Taguchi et al., 2010). These enzymes can catalyze the transfer of a malonyl group from malonyl coenzyme A (CoA) to the phenolic glycosides and play an important role in various processes, including xenobiotic detoxification (Taguchi et al., 2005, 2010). Certain specialized insects, in particular those that feed on trees of the Salicaceae, can also readily cope with phenolic glycosides and may even use them as feeding and oviposition stimulants (Boeckler et al., 2011). They neutralize the defensive phenolic glycosides either by using specific detoxifying enzymes, decreasing the enzyme activity of β-glucosidases, directly sequestering phenolic glycosides, or converting them to salicylaldehyde (Boeckler et al., 2011; Després et al., 2007; Opitz and Müller, 2009). However, the mechanisms that allow generalist insects with a broad range of host plants to overcome the effects of phenolic glycosides are unknown.

The sweet potato whitefly, *Bemisia tabaci* (Gennadius), is a species complex of at least 30 cryptic species, some of which (e.g., Mediterranean [MED] and Middle East-Asia Minor 1 [MEAM1]) are among the most devastating crop pests (De Barro et al., 2011; Liu et al., 2007). Outbreaks occur often worldwide, and *B. tabaci* can seriously reduce crop yields by feeding on phloem, transmitting plant viruses, and excreting honeydew (Gilbertson et al., 2015). It is extremely polyphagous—more than 600 host plant species have been recorded—and exhibits

exceptional host adaptability (Oliveira et al., 2001). Most of its host plants contain phenolic glycosides, and uncovering how *B. tabaci* copes with these defense metabolites could help explain its pervasive host adaptability.

Here, using bioinformatic, molecular, and biochemical approaches, combined with insect performance assays, we show that the *B. tabaci* genome harbors a plant-specific and horizontally transferred gene, *BtPMaT1*, encoding a phenolic glucoside malonyltransferase that enables the detoxification of phenolic glycosides. This discovery reveals an unexpected route by which *B. tabaci* has evolved its extraordinary ability to overcome the defenses of its host plants. Moreover, we show that interfering with the functioning of this plant-derived gene in *B. tabaci* can be a highly effective way to control this extremely important global pest.

RESULTS

Identification and characterization of malonyltransferase genes in *B. tabaci*

Based on a preliminary survey of *B. tabaci* MED genes related to KEGG (Kyoto Encyclopedia of Genes and Genomes) pathways, we identified the *BtPMaT1* gene (*BTA023005.1*). This gene consists of one exon (Figure 1A) and was cloned from *B. tabaci* MED adults using specific PCR primers (Table S1). The coding sequence (CDS) of the *BtPMaT1* gene (GenBank: MN756010) spans 1,386 nucleotides and encodes a protein of 461 amino acids that lacks an N-terminal signaling peptide (Figure S1A). Compared with BTA023005.1, the cloned *BtPMaT1* CDS contained several non-synonymous single-nucleotide polymorphisms (Figure S1B). A BLASTp search against the predicted protein dataset of the *B. tabaci* MED genome (http://gigadb.org/dataset/100286) (Xie et al., 2017) revealed the presence of BTA005164.2 (BtPMaT2), a close homolog of BtPMaT1 (BLASTp E-value of 7.9E−107). Both *B. tabaci* MED proteins carried the conserved HXXXD and DFGWG motifs of plant BAHD acyltransferases (named according to the first letter of each of the first four biochemically characterized enzymes of this family [BEAT, AHCT, HCBT and DAT]) (D'Auria, 2006). The YXGNC motif, typical for phenolic glycoside and anthocyanin malonyltransferases (belonging to "clade I" BAHD acyltransferases) (D'Auria, 2006; Tuominen et al., 2011; Zhao et al., 2011), was also present (Figure S2). In this study, we primarily investigated the potential role of BtPMaT1 in the detoxification of phenolic glycosides, and whether BtPMaT2 also plays a potential role in neutralizing plant metabolites remains to be determined.

Evidence for the horizontal transfer of *BtPMaT1* from plants to whiteflies

BLASTp and tBLASTn searches against the NCBI non-redundant database revealed that BtPMaT1 had its closest homologs in plants (E-value < E−90, bit-score > 300) and did not have homologs in other arthropods, except for other *B. tabaci* cryptic species (e.g., XP_018897056.1/Bta07786 in *B. tabaci* MEAM1) (Figure 1D; Figure S3). An InterProScan search (Jones et al., 2014) of BtPMaT1 revealed the presence (E-value of 1.7E−110) of the PANTHER domain PTHR31625, which has to date only been detected in plant and fungal proteins (3,073 sequences) and one bacterial protein (GenBank: KPK61911) (see "Taxonomy" tab at https://www.ebi.ac.uk/interpro/entry/panther/PTHR31625/, accessed on November 15, 2020). Last, a maximum likelihood phylogenetic analysis showed that BtPMaT1 clustered within a group of plant BAHD acyltransferases containing the PTHR31625 domain and the YXGNC motif (Figure 1B, Figure S4; Data S1).

Independent genomic analyses were then performed to confirm that *BtPMaT1* is indeed integrated into the *B. tabaci* MED genome. We found that *BtPMaT1* is located on scaffold 523 surrounded by two typical arthropod serine protease genes (*BTA023004.3* and *BTA023006.1*), both of which contains 9 exons (Figure 1D). Identical neighboring genes were also found for *BtPMaT1* in the *B. tabaci* MEAM1 genome (Figure 1D), whereas no ortholog of *BtPMaT1* was found in the region near a gene of the greenhouse whitefly, *Trialeurodes vaporariorum* (*Tv04085* on scaffold 2), that was the most homologous to the two flanking *B. tabaci* serine proteases genes (both XP_018897238.1/Bta07787 and XP_018897055.1/Bta07785 of *B. tabaci* MEAM1 had their best BLASTp hit with Tv04085 [E-value of E−163 and E−58, respectively]). It was also not found in any other region of the *T. vaporarorium* genome. PCR confirmed that *BtPMaT1* was integrated between the two serine protease genes in the *B. tabaci* MED genome (Figure 1C). Despite an uneven coverage of New World *B. tabaci*, the coverage was highly consistent in the *BtPMaT1* gene region among different *B. tabaci* cryptic species (Figure 1A). Finally, the expression of *BtPMaT1* was detected in all strains of *B. tabaci* MED that were reared on different host plants (Figure 1E), indicating the presence of *BtPMaT1* is independent of *B. tabaci* strain and host plant. Overall, our analyses show that the *BtPMaT1* gene is not a plant gene contaminant and strongly indicate that *BtPMaT1* has been horizontally acquired from plants.

The spatio-temporal expression profiling of the *BtPMaT1* gene

The spatio-temporal expression pattern of *BtPMaT1* was monitored with real-time quantitative PCR (qPCR) using five developmental stages (eggs, 1st–2nd, 3rd, and 4th instar nymphs, adults) and various parts of the adults (head, thorax, abdomen, non-gut tissue, and gut tissue) of *B. tabaci* MED. This showed that *BtPMaT1* was expressed in all developmental stages and tissues (Figures S5A–S5C). The significantly higher expression in adults suggests that *BtPMaT1* plays its most important role in the adult stage. Moreover, *BtPMaT1* was most highly expressed in the abdomen and especially in the gut, which indicates that it is a gut-specific gene that plays a key role in detoxification processes. Remarkably, *BtPMaT1* expression was, albeit to a much lesser extent, also detected in the egg stage, providing additional evidence that the *BtPMaT1* gene is not a plant gene contaminant.

Phenolic glycosides in tomato leaves and effect of phenolic glycosides on *B. tabaci* performance

To test whether the *BtPMaT1* gene is indeed involved in the metabolism of phenolic glycoside in host plants, we first determined the classes of phenolic glycosides in tomato leaves using

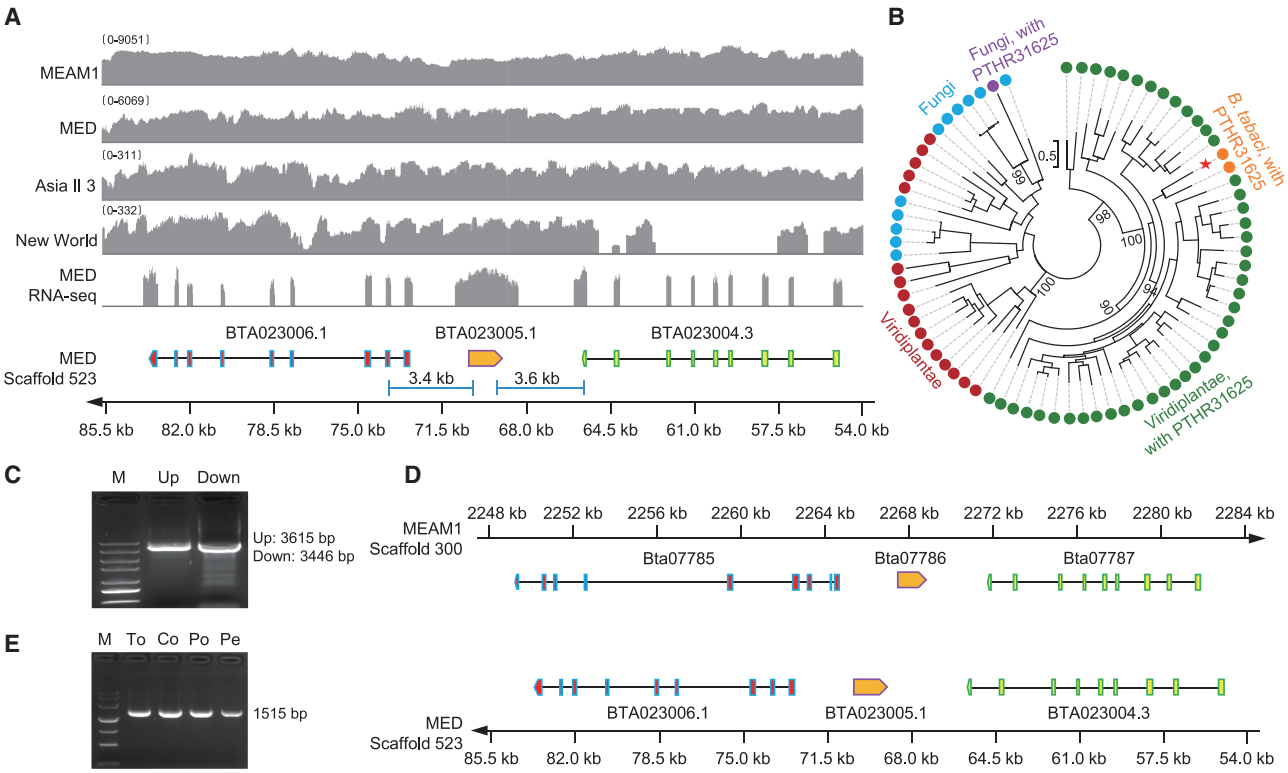

Figure 1. Evidence for the horizontal transfer of *BtPMaT1* in *B. tabaci*

(A) Genomic location of *BtPMaT1* (*BTA023005.1*) and its adjacent genes (*BTA023004.3* and *BTA023006.1*) in *B. tabaci* MED. Genomic fragments cloned by PCR are indicated in blue. Illumina DNA-read coverage plots derived from genomic sequencing of different *B. tabaci* cryptic species and an Illumina RNA sequencing (RNA-seq) read coverage plot from adult *B. tabaci* MED are shown. The sequence depths are indicated by the numbers between brackets.

(B) Maximum likelihood phylogenetic analysis of BtPMaT1. BtPMaT1 of *B. tabaci* clusters, together with BtPMaT2, within a group of plant BAHD acyltransferases containing the PTHR31625 domain. The tree is midpoint rooted, and the scale bar represents 0.5 amino acid substitutions per site. Only bootstrap values at phylogenetically important nodes are shown. BtPMaT1 is indicated by a red star.

(C) Genome fragments cloned from *B. tabaci* MED. M, marker (from top to bottom: 4,000 bp, 3,500 bp, 3,000 bp, 2,500 bp, 2,000 bp, 1,500 bp, 1,000 bp); Up, *BTA023004.3-BtPMaT1* genome fragment; Down, *BtPMaT1-BTA023006.1* genome fragment.

(D) Genome synteny of the *BtPMaT1* gene and its two surrounding serine protease genes in *B. tabaci* MED and *B. tabaci* MEAM1. The reverse complement of the *B. tabaci* MED genomic fragment was taken for ease of showing the genome synteny.

(E) PCR products of *BtPMaT1* obtained from *B. tabaci* MED feeding on different hosts. M, marker (from top to bottom: 4,500 bp, 3,000 bp, 2,000 bp, 1,200 bp, 800 bp, 500 bp, 200 bp). Co, cotton; Pe, pepper; Po, poinsettia; To, tomato. See also Figures S1, S2, S3, and S4; Table S1; and Data S1.

ultra-performance liquid chromatography/quadrupole time-of-flight mass spectrometry (UPLC-QTOF/MS). The experimental process as shown in Figure 2A resulted in UV and MS spectra (Figures 2B and 2C) that detected a total of 9,873 metabolites, and 6,005 compounds were identified by Progenesis QI analysis. Among them, 290 were identified as phenolic glycosides by manual filtering (Figure 2D; Table S2). Following a previous study (Lattanzio et al., 2006), the phenolic glycosides were assigned to 9 categories based on their basic skeleton dominated by C_6–C_3–C_6 glycosides (Figure 2E; Table S2). Subsequently, 11 representative phenolic glycosides from each category, present in a variety of different plant species, were selected (Figure 2; Table S2) to explore their possible impact on the performance of *B. tabaci* adults. Bioassay results demonstrated that the adult mortality caused by five of the phenolic glycosides (kaempferol 3-O-glucoside, kaempferol 7-O-glucoside, phenyl β-D-glucoside, phlorizin, and rhaponticin) was significantly higher than the control, whereas mortality caused by the remaining six compounds (4-nitrophenyl β-D-glucoside, salicin, androsin, verbascoside, 4-methylumbelliferone glucoside, and polygalaxanthone III) was not significantly different from the control (Figure 3B), implying that several phenolic glycosides are toxic to *B. tabaci* when ingested at a dose (10 μM) that is higher than what they are normally exposed to when feeding on plant phloem.

Functional analysis of the *BtPMaT1* gene using RNAi and VIGS assays

To validate the role of *BtPMaT1* in phenolic glycoside detoxification, we performed dietary RNA interference (RNAi) by directly feeding its specific double-stranded RNA (dsRNA) (dsBtPMaT1) to *B. tabaci* MED adults (Figure 3A). qPCR analysis at 48 h post-RNAi showed that *BtPMaT1* expression was reduced by 49.2% compared with the control (Figure 3C). Silencing *BtPMaT1* gene had no direct effect on *B. tabaci* survival (Figure 3D). Subsequent feeding assays revealed that silencing of *BtPMaT1* significantly increased the mortality of adults feeding on

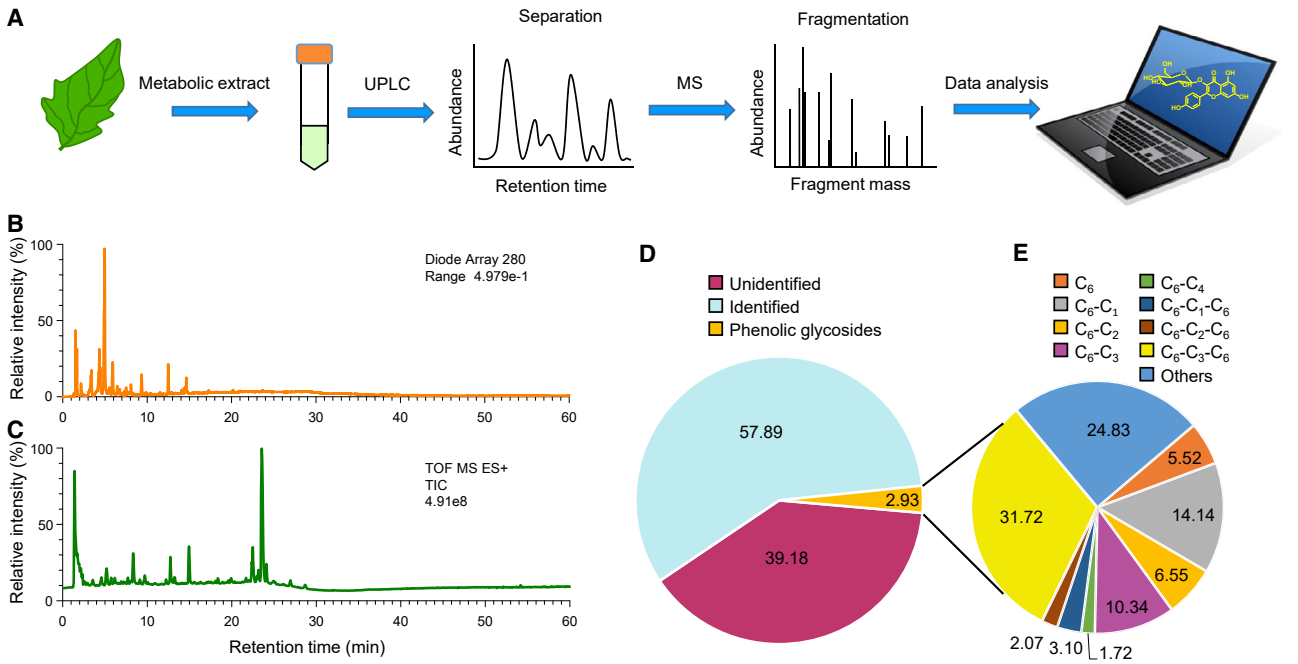

Figure 2. Metabolite profiling of tomato leaves

(A) Procedure for UPLC-QTOF/MS analysis of metabolite extract from tomato leaves. Tomato leaves were frozen and ground into powder. The metabolites were extracted with methanol/formic acid (9:1, v/v) and were analyzed using the ACQUITY UPLC I-Class/Xevo G2-XS QTOF system.

(B) UV chromatograms obtained at 280 nm.

(C) Mass spectra were obtained with positive-ion mode.

(D) Classification of 9,873 metabolites from tomato leaves.

(E) Categories of phenolic glycosides detected by manual filtering. See also Table S2.

kaempferol 3-*O*-glucoside (Figure 3E), kaempferol 7-O-glucoside (Figure 3F), or rhaponticin (Figure 3G), but did not significantly increase the mortality of adults feeding on phenyl β-D-glucoside (Figure 3H) or phlorizin (Figure 3I). This result confirms that *BtPMaT1* plays a pivotal role in the detoxification of some, but not all, detrimental phenolic glycosides.

Subsequently, we further tested the function of *BtPMaT1* in an ecologically relevant experiment, with whitefly adults actually feeding on plants and using a virus-induced gene silencing (VIGS) technique. We first cloned specific gene-silencing fragments into the pTRV2 vector to construct the VIGS vectors pTRV2-BtPMaT1 and pTRV2-EGFP (Figure 3J). pTRV1 and recombinant pTRV2-BtPMaT1 and pTRV2-EGFP were then introduced into *Agrobacterium tumefaciens*. Equal volumes of *A. tumefaciens* containing pTRV1 and pTRV2 harboring the target gene were mixed and infiltrated into two true leaves of tomato plants using a needleless syringe (Figure 3K). After 20 days, silencing fragments of the *BtPMaT1* gene and the *EGFP* gene were detected in the tomato seedlings by PCR (Figures 3L and 3M). Next, *BtPMaT1* expression in *B. tabaci* adults that had been feeding on the tomato seedlings for 7 days was assessed by qPCR. Relative to expression in adults feeding on pTRV2-EGFP tomato plants, *BtPMaT1* expression in adults feeding on pTRV2-BtPMaT1 tomato plants was reduced by 63.8% (Figure 3N). Moreover, continuous silencing of *BtPMaT1* by VIGS for 7 days significantly increased mortality and reduced fecundity of *B. tabaci* adults (Figures 3O and 3P).

The BtPMaT1 protein metabolically detoxifies phenolic glycosides

To confirm that BtPMaT1 is indeed able to acylate phenolic glycosides, *BtPMaT1* was heterologously expressed in *Spodoptera frugiperda* (Sf9) cells (Figure S6) for *in vitro* enzyme activity tests. UPLC-QTOF/MS analyses showed that the recombinant BtPMaT1 protein has malonyltransferase activity against three of the eleven tested phenolic glycosides: kaempferol 3-O-glucoside, kaempferol 7-O-glucoside, and rhaponticin. Each was converted into their respective malonylglucoside (Figure 4), with a higher activity to the flavonoid substances kaempferol 7-O-glucoside and kaempferol 3-O-glucoside than to the non-flavonoid rhaponticin (Figure 5B). Flavonoids are very abundant in plants, in particular kaempferol, quercetin, apigenin, and naringenin, which mainly exist in a glycosylated state. Based on our results, we hypothesize that BtPMaT1 is able to malonylate flavonoids other than kaempferol glucoside, which we confirmed for isoquercetin (quercetin 3-O-β-D-glucopyranoside), apigetrin (apigenin-7-O-glucoside), and prunin (naringenin-7-O-glucoside) (Figures 4 and 5B). Moreover, we also confirmed the acylation activity of BtPMaT1 *in vivo*, observing that kaempferol 3-O-glucoside, kaempferol 7-O-glucoside, rhaponticin, isoquercetin, apigetrin, or prunin were metabolized when they were incubated with the dissected and pooled

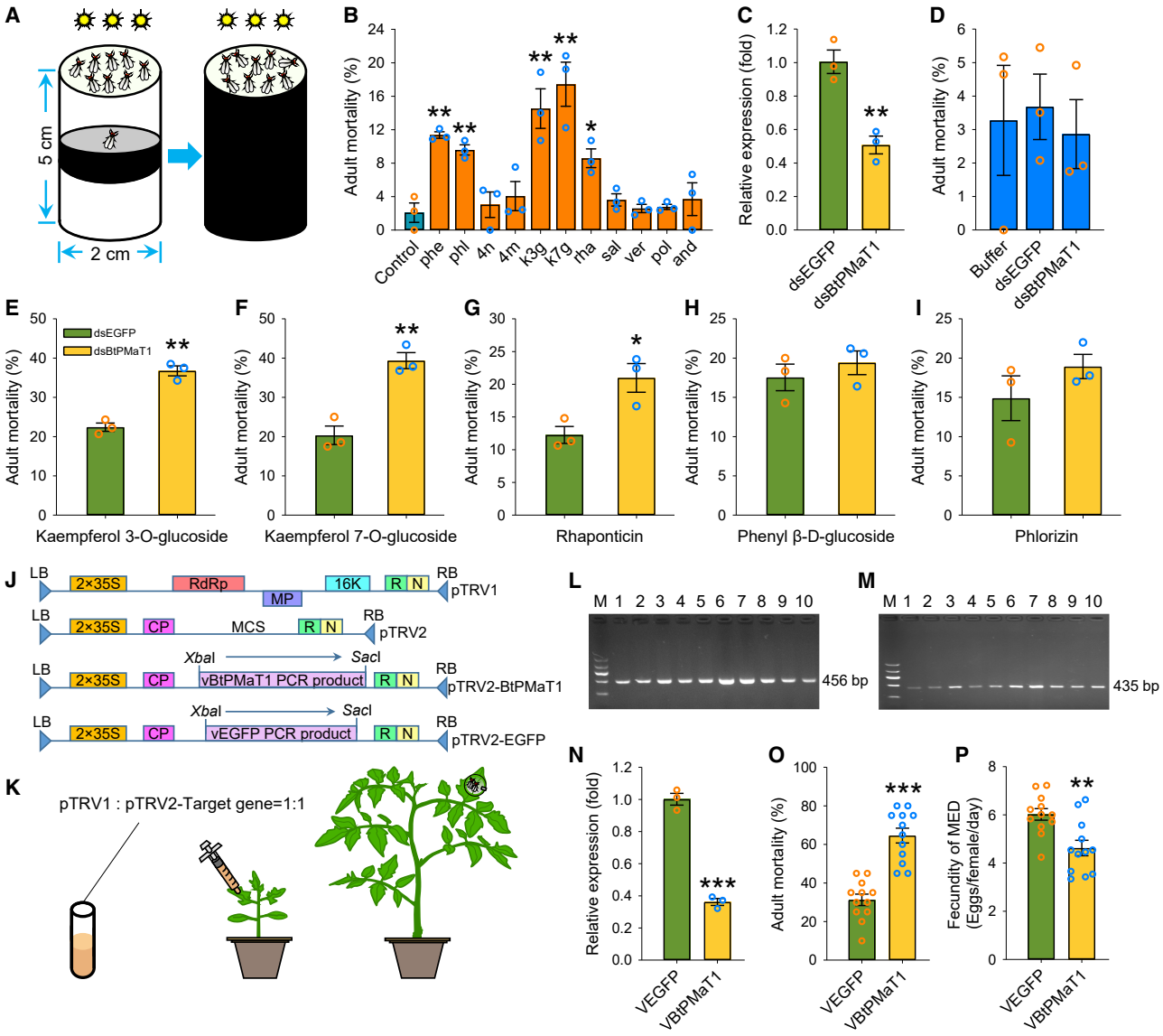

Figure 3. Effect of *BtPMaT1* silencing on *B. tabaci* performance

(A) A diagram of the whitefly dsRNA feeding setup. The diet containing dsRNA was placed between two Parafilm layers at the top end of a glass feeding tube (2 cm in diameter × 5 cm in length). After placing whiteflies into the tube from its bottom end, the tube was then sealed with a black cotton plug, covered with a black tube sleeve, and with the Parafilm-covered top end oriented toward a light source at ~20 cm distance.

(B) Effects of phenolic glycosides on the mortality of non-silenced *B. tabaci* adults recorded at 96 h. phe, phenyl β-D-glucoside; phl, phlorizin; 4n, 4-nitrophenyl β-D-glucoside; 4m, 4-methylumbelliferone glucoside; rha, rhaponticin; sal, salicin; k3g, kaempferol 3-O-glucoside; k7g, kaempferol 7-O-glucoside; ver, verbascoside; pol, polygalaxanthone III; and, androsin.

(C) The transcript levels of *BtPMaT1* at 48 h post-RNAi as determined by qPCR.

(D) The adult mortality of *B. tabaci* after *BtPMaT1* gene silencing.

(E–I) Effects of *BtPMaT1* silencing on mortality of *B. tabaci* adults feeding on different phenolic glycosides for 96 h.

(J) The constructed TRV-based VIGS vectors.

(K) Procedure for persistent gene silencing of *B. tabaci* using TRV-based vectors.

(L and M) PCR products amplified using cDNA from pTRV2-BtPMaT1 (L) and pTRV2-EGFP (M) tomato leaves treated for 20 days. M, marker (from top to bottom: 1,200 bp, 900 bp, 700 bp, 500 bp, 300 bp, 100 bp); lanes 1–10, PCR products (L, 456-bp dsBtPMaT1 fragment; M, 435-bp dsEGFP fragment).

(N) The transcript levels of *BtPMaT1* in *B. tabaci* adults feeding on pTRV2-BtPMaT1 tomatoes for 7 days as determined by qPCR.

(O and P) Male/female adult mortality (O) and female adult fecundity (P) of *B. tabaci* feeding on pTRV2-BtPMaT1 tomatoes and pTRV2-EGFP tomatoes for 7 days. Values are means ± SEM, n = 3 (B–I and N) and n = 12 (O and P) biologically independent samples, *p < 0.05, **p < 0.01, ***p < 0.001 one-way ANOVA with Holm-Sidak's test was used for comparison. See also Table S1.

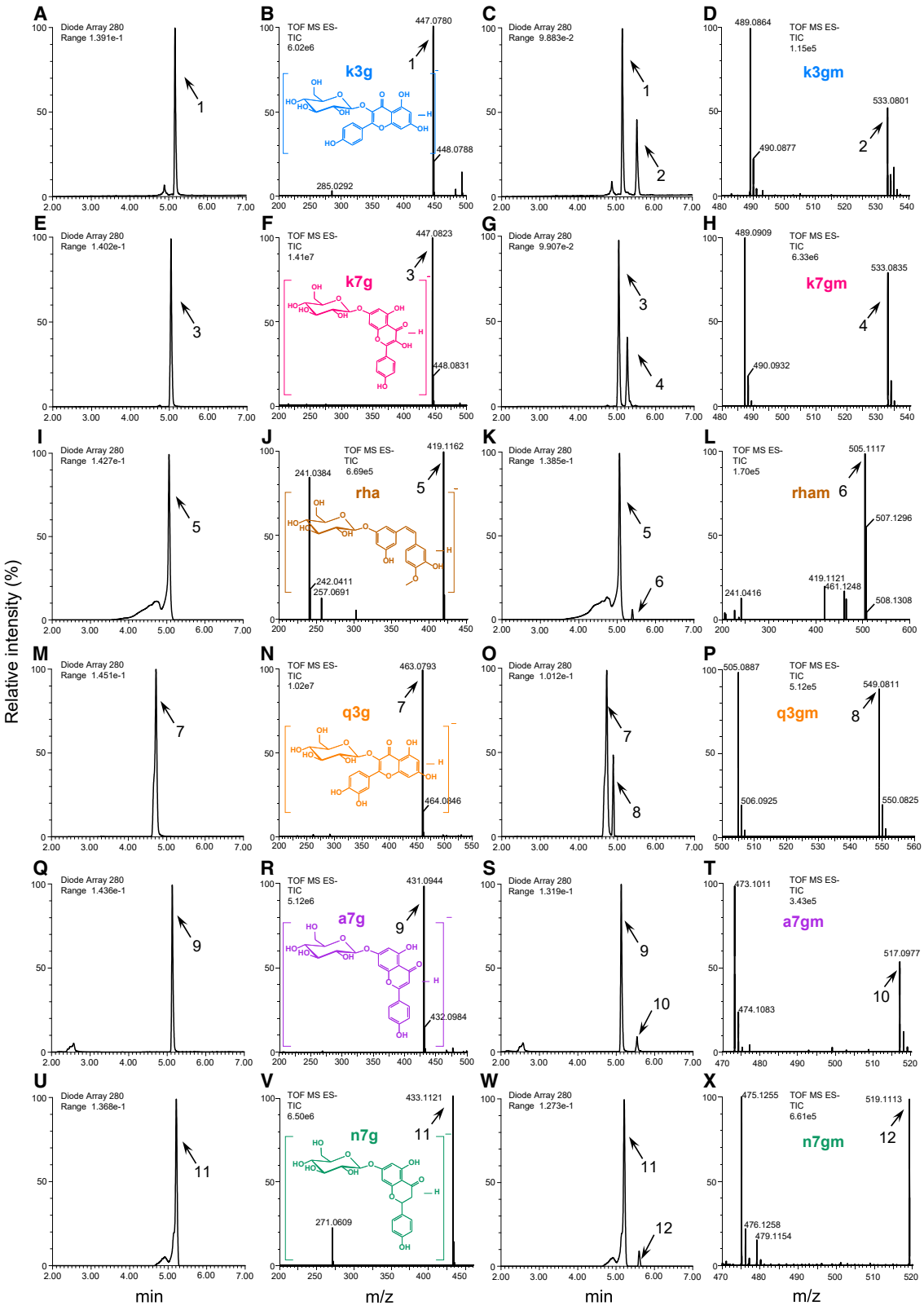

(legend on next page)

B. tabaci adult gut tissues (Figure 5C). This further confirms the expected metabolic function of the BtPMaT1 protein and suggests that the malonylation reaction occurs inside the *B. tabaci* adult gut tissues.

To further test whether BtPMaT1 can *in vivo* metabolize phenolic glycosides in *B. tabaci*, we collected the honeydew after oral feeding of a representative phenolic glycoside and after feeding on transgenic tomatoes (Figure 5A). After *B. tabaci* adults were fed a representative phenolic glycoside (kaempferol 3-O-glucoside) for 48 h, kaempferol 3-O-glucoside and malonylated kaempferol 3-O-glucoside were found in the honeydew (Figures 5E and 5F). Moreover, silencing of *BtPMaT1* by oral delivery of its specific dsRNA significantly increased kaempferol 3-O-glucoside and decreased malonylated kaempferol 3-O-glucoside in honeydew (Figures 5G and 5H), supporting the notion that BtPMaT1 catalyzes malonylation of phenolic glycosides *in vivo* in *B. tabaci*. The role of malonylation of phenolic glycosides catalyzed by the BtPMaT1 protein in a metabolic detoxification process was further validated by feeding *B. tabaci* adults on diet solution with kaempferol 3-O-glucoside and the corresponding phenolic malonylglycoside [kaempferol 3-O-(6-malonyl-glucoside)] (Figure 5D). Mortality of *B. tabaci* adults fed on kaempferol 3-O-glucoside was significantly higher than those fed on control diet. By contrast, the kaempferol 3-O-(6-malonyl-glucoside) diet had a far less lethal effect, further confirming the important role of malonylation catalyzed by BtPMaT1 in the detoxification of phenolic glucosides. We also performed a whole-metabolome assay of the honeydew of *B. tabaci* fed on wild-type and transformed tomato plants that silence the *BtPMaT1* gene, as described in the next section. As shown in Figure 5I and Tables S3 and S4, a total of 2,966 metabolites were detected in the whitefly honeydew, and 94 flavonoid glycosides and 4 flavonoid malonylglucoside compounds could be identified. Among them, the relative levels of 50 flavonoid glycosides were significantly higher in the honeydew of *B. tabaci* fed on transformed tomato plants, while the four detected flavonoid malonylglucosides were significantly lower, supporting the phenolic glucoside malonyltransferase function of the *BtPMaT1* gene.

The transgenic expression of dsBtPMaT1 in tomato enhances resistance to whiteflies

A final experiment was conducted to validate the notion that impairing *BtPMaT1* in *B. tabaci* can enhance plant resistance to the pest. Hairpin RNA of *BtPMaT1* was produced by transcription of two inverted repeats of 444-bp target fragment of *BtPMaT1*. The transfer DNA (T-DNA) region of the hairpin RNA expression vector (pCAMBIA-RNAi-*BtPMaT1*) as shown in Figure S7A was transferred to tomato using *A. tumefaciens*-based genetic transformation (Figures S7B–S7F). Positive transgenic lines were identified by PCR amplification (Figure 6A). Northern blot analyses confirmed that positive transgenic lines contained both long dsRNAs and small interfering RNAs (siRNAs) of *BtPMaT1* (Figure 6B). Gene-silencing efficiency in whitefly adults was confirmed by qPCR and showed that 7 days of feeding on transgenic tomatoes significantly reduced *BtPMaT1* expression compared with the control (Figure 6C). Mortality of whiteflies was already higher after 1 day of feeding on transgenic tomatoes and increased over time (Figure 6D). Most importantly, in field simulation cages, feeding on transgenic tomatoes results in almost 100% mortality of whiteflies compared with less than 20% in the control (Figures 6E, 6J, and 6K). By contrast, the performance of a non-target insect, the peach-potato aphid, *Myzus persicae* (Hemiptera: Aphididae), was unaffected on transgenic plants after 7 days of feeding in both clip cages (Figure 6F) and field simulation cages (Figures 6G, 6L, and 6M). Likewise, the mortality of another non-target arthropod pest, the spider mite *Tetranychus urticae* (Acarina: Tetranychidae) was unaffected after 7 days of feeding on transgenic plants either in individual leaf assays in Petri dishes (Figure 6H) or on whole plants (Figures 6I, 6N, and 6O).

DISCUSSION

The ability of herbivorous insects to detoxify plant defense compounds is pivotal for their adaptive evolution (Heidel-Fischer and Vogel, 2015), and it is increasingly evident that the modification of secondary metabolites by detoxifying enzymes is a highly effective strategy to neutralize plant toxins, also applied by whiteflies (Malka et al., 2020). The above-mentioned experiments reveal an uncommon evolutionary route by which whiteflies have gained the ability to malonylate a common group of plant defense compounds through the acquisition of a plant detoxification gene. The horizontal transfer of *BtPMaT1* is shown to empower whiteflies with the ability to attach a malonyl group to phenolic glucosides, rendering these common plant-produced secondary metabolites almost completely innocuous (Figure 7). The metabolic detoxification process in *B. tabaci* most likely relies on a conjugation reaction similar to herbicide metabolism in certain plants, whereby malonyltransferase can catalyze detoxification by conjugating the herbicide or an intermediate metabolite with malonyl-CoA (Frear et al., 1983; Lao et al., 2003). Moreover, BtPMaT1 malonylation might promote the solubility and export of the ingested phenolic glycosides (Taguchi et al., 2010; Zhao, 2015). BtPMaT1 malonylation might also prevent glucosidase action on phenolic glycosides, as previously shown for malonylation of anthocyanins (Suzuki et al.,

Figure 4. Metabolic analyses of BtPMaT1 enzyme activity

(A–X) BtPMaT1 protein expressed by Sf9 cells catalyzes the malonylation of kaempferol 3-O-glucoside (A–D), kaempferol 7-O-glucoside (E–H), rhaponticin (I–L) quercetin 3-O-β-D-glucoside (M–P), apigenin-7-O-glucoside (Q–T), and naringenin-7-O-glucoside (U–X). 1, [kaempferol 3-O-glucoside -H]$^-$; 2, [kaempferol 3-O-malonylglucoside -H]$^-$; 3, [kaempferol 7-O-glucoside -H]$^-$; 4, [kaempferol 7-O-malonylglucoside -H]$^-$; 5, [rhaponticin -H]$^-$; 6, [rhaponticin malonylglucoside -H]$^-$; 7, [quercetin 3-O-β-D-glucoside -H]$^-$; 8, [quercetin 3-O-β-D-malonylglucoside -H]$^-$; 9, [apigenin-7-O-glucoside -H]$^-$; 10, [apigenin-7-O-malonylglucoside -H]$^-$; 11, [naringenin-7-O-glucoside -H]$^-$; 12, [naringenin-7-O-malonylglucoside -H]$^-$. Abbreviations are as follows: k3g, kaempferol 3-O-glucoside; k3gm, kaempferol 3-O-malonylglucoside; k7g, kaempferol 7-O-glucoside; k7gm, kaempferol 7-O-malonylglucoside; rha, rhaponticin; rham, rhaponticin malonylglucoside; q3g, quercetin 3-O-β-D-glucoside; q3gm, quercetin 3-O-β-D-malonylglucoside; a7g, apigenin-7-O-glucoside; a7gm, apigenin-7-O-malonylglucoside; n7g, naringenin-7-O-glucoside; and n7gm, naringenin-7-O-malonylglucoside. See also Figure S6.

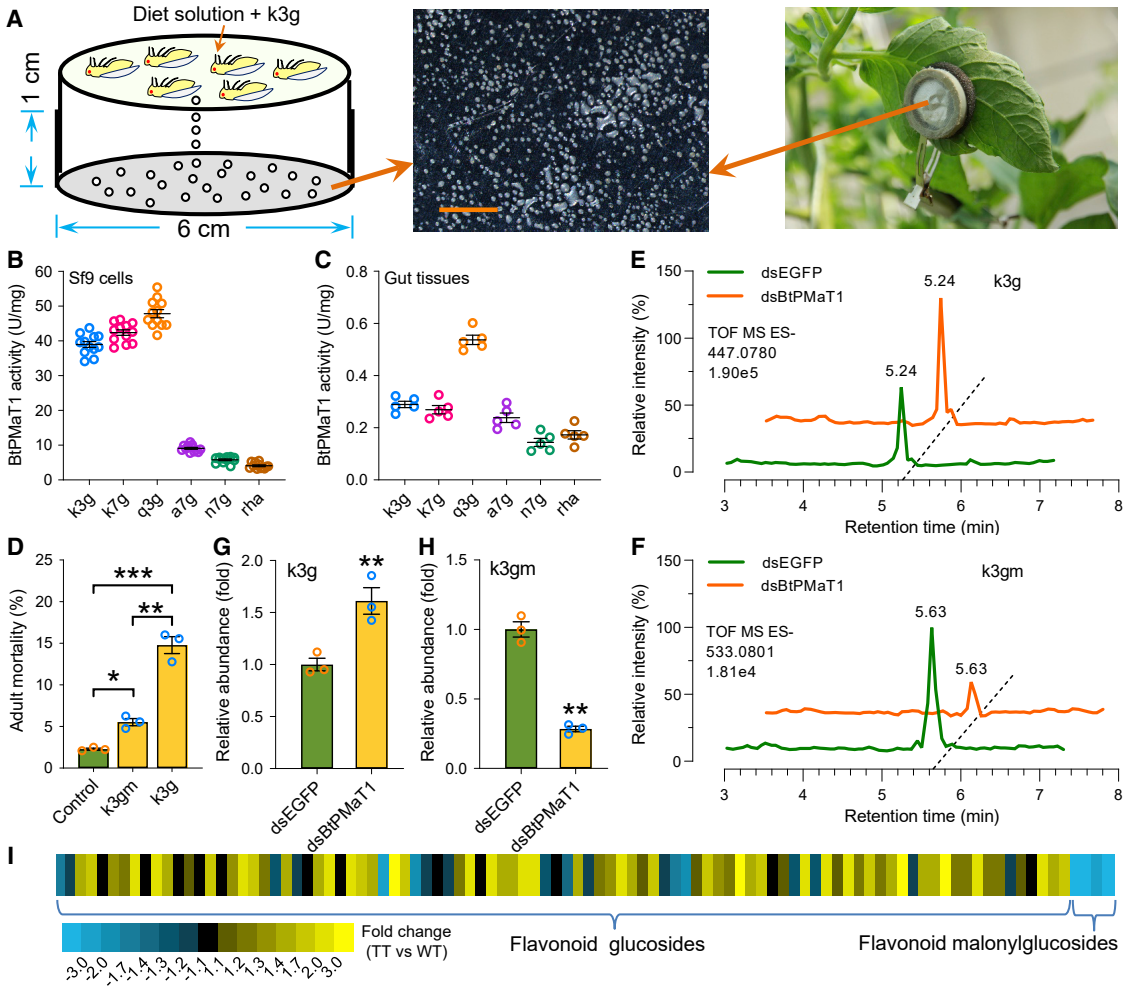

Figure 5. BtPMaT1 metabolizes phenolic glycosides

(A) Illustration of the whitefly honeydew collection setup. The honeydew collection device consists of a vertically oriented plastic tube (6 cm in diameter × 1 cm in length) and a plastic bottom covered with tinfoil. Scale bar, 1 mm.

(B–D) The enzyme activity of BtPMaT1 protein and the validation of its role in detoxification of phenolic glycosides. (B and C) Specific enzyme activity was measured of protein BtPMaT1 expressed in Sf9 cells (B) and gut tissues (C). (D) Effects of a representative phenolic glycoside k3g and its conjugated metabolite k3gm on *B. tabaci* mortality. Adult mortality of *B. tabaci* was recorded after the adults fed on diet solutions without any phenolic glycosides (control), diet solution with the k3g, or diet solution with k3gm for 96 h.

(E–H) Effects of *BtPMaT1* silencing on k3g metabolism of *B. tabaci*. Quantities of k3g (E) and k3gm (F) were measured for honeydew collected from whiteflies fed dsEGFP or dsBtPMaT1, and significant differences for k3g (G) and k3gm (H) were determined. (I) Metabolites in honeydew collected from whiteflies that fed on wild-type (WT) tomato or tomato expressing dsBtPMaT1 (TT) were analyzed by UPLC-QTOF/MS. Fold changes of phenolic glycoside levels in TT compared with WT are depicted using a heatmap. k3g, kaempferol 3-O-glucoside; k3gm, kaempferol 3-O-malonylglucoside; k7g, kaempferol 7-O-glucoside; q3g, quercetin 3-O-β-D-glucoside; a7g, apigenin-7-O-glucoside; n7g, naringenin-7-O-glucoside; rha, rhaponticin. Values are means ± SEM, n = 12 (B), n = 5 (C), and n = 3 (D–H) biologically independent samples, *p < 0.05, **p < 0.001, ***p < 0.001 one-way ANOVA with Holm-Sidak's test used for comparison. See also Tables S1, S3, and S4.

2002), and hence, reminiscent of adaptation mechanisms reported for insects feeding on Salicaceae, possibly limits the release of the (more) toxic aglycones (Ahmad et al., 1986; Lindroth, 1988). Intriguingly, our phylogenetic analyses showed that BtPMaT1 not only clustered with several plant phenolic glucoside malonyltransferases (AtPMaT1, AtPMaT2, Vh3MaT1, Lp3MaT1, and NtMaT1) but also with isoflavone glucoside (GmIMaT3, GmMaT4, and MtMaT4) and anthocyanin (Ss5MaT1) malonyltransferases (Figure S4), implying that additional substrates might be malonylated by BtPMaT1. Together with the presence of BtPMaT2 (Figure 1B; Figure S4), this likely broadens the spectrum of defensive compounds that can be neutralized by *B. tabaci*, warranting further study.

The heterologous expression of BtPMaT1 protein in Sf9 cells was found to catalyze the malonylation of phenolic glucosides (especially flavonoid glucosides). The malonylated product was detected in the honeydew after *B. tabaci* fed on kaempferol 3-O-glucoside, while suppressing the *BtPMaT1* gene expression

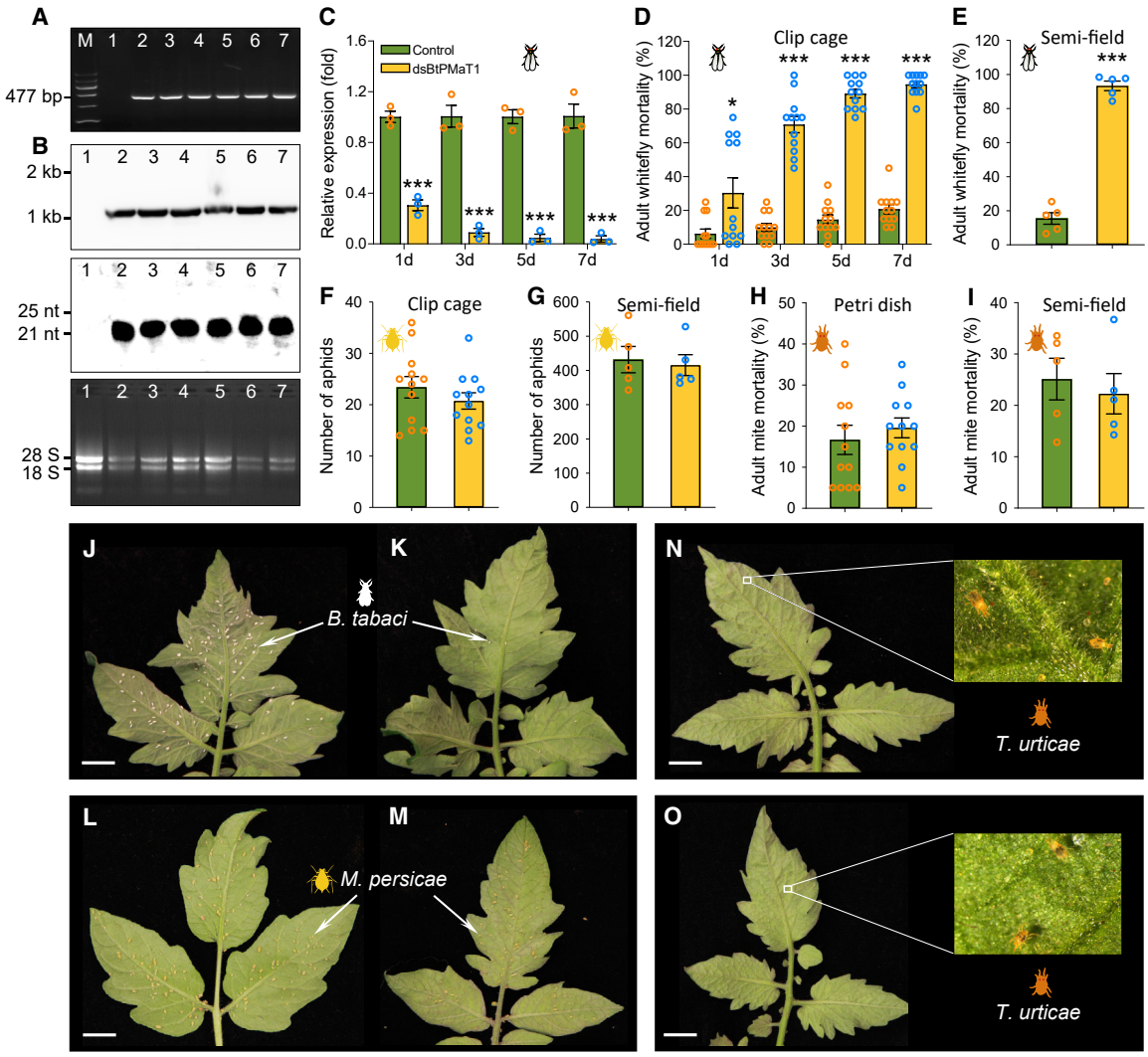

Figure 6. Transgenic tomato plants expressing dsBtPMaT1 are resistant to *B. tabaci*

(A) PCR analysis for *BtPMaT1* putative transgenic tomatoes. M, marker (from top to bottom: 1,200 bp, 900 bp, 700 bp, 500 bp, 300 bp, 100 bp); lane 1, negative control; lanes 2–7, transgenic tomatoes.

(B) Northern blot analysis of long dsRNA (top box) and siRNA (middle box) produced by positive transgenic tomatoes. GoldView-stained total RNAs are shown (bottom box).

(C) Silencing effect of feeding on transgenic tomatoes on *BtPMaT1* expression in whitefly adults.

(D) Lethal effect of transgenic tomatoes on *B. tabaci* determined using clip cages.

(E, G, and I) The mortality of *B. tabaci* (whitefly) (E) and *T. urticae* (spider mite) (I) and the number of *M. persicae* (peach-potato aphid) (G) feeding on transgenic tomatoes for field-simulated bioassays.

(F and H) The number of *M. persicae* (F) and the mortality of *T. urticae* (H) feeding on transgenic tomatoes. Values are means ± SEM, n = 3 (C), n = 5 (E, G, and I), and n = 12 (D, F, and H) biologically independent replicates, *p < 0.05, ***p < 0.001 one-way ANOVA with Holm-Sidak's test used for comparison.

(J–O) Effect of transgenic tomatoes on the fitness of *B. tabaci* (J and K), *M. persicae* (L and M), and *T. urticae* (N and O) in field-simulated bioassays. Scale bars, 1 cm. See also Figure S7 and Table S1.

significantly decreased levels of this glucoside in the honeydew of *B. tabaci*. Moreover, we detected specific *BtPMaT1* expression and malonyltransferase activity of BtPMaT1 inside the gut tissue. The enzyme possesses no signal peptide and must mainly exert its function in the cytosol of the gut cells rather than in the gut lumen. Hence, flavonoid glucosides need to enter the gut cells first, which might require a similar transport mechanism as in mammals. In mammals, one type of flavonoid glucoside can be directly transported into the gut cells by the sodium-dependent glucose transporter 1 (SGLT1) located on the cell membrane (Walle, 2004). The other group of flavonoid glucosides first needs to be hydrolyzed into flavonoids in the gut lumen and then absorbed into gut cells by passive diffusion (Terahara, 2015). UDP-glucuronosyltransferases (UGTs) are known to catalyze glucuronic acid conjugation of flavonoids to produce flavonoid glucosides in mammalian gut cells (Walle, 2004). Considering that

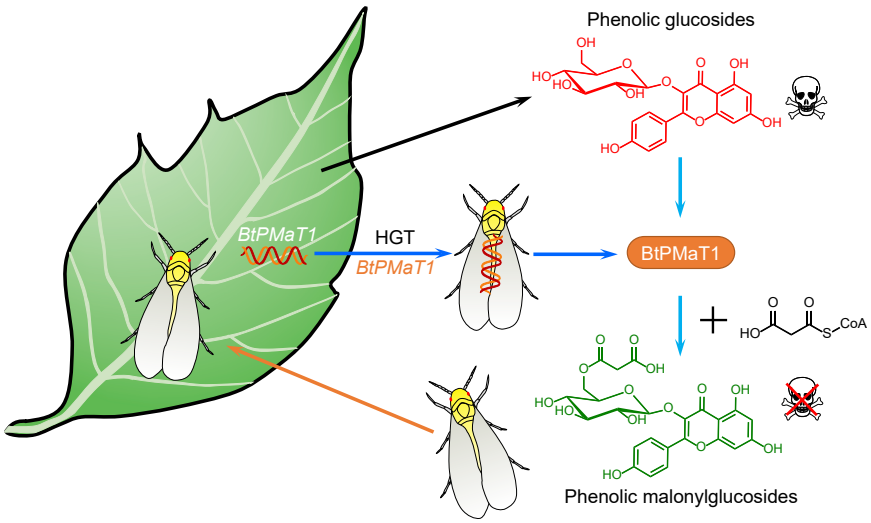

Figure 7. Schematic overview of how the acquisition of the plant gene *BtPMaT1* empowers the whitefly *B. tabaci* to neutralize plant phenolic glycosides

BtPMaT1 is a phenolic glucoside malonyltransferase gene horizontally transferred from plants to *B. tabaci*. In *B. tabaci*, malonylation of phenolic glycosides is catalyzed by BtPMaT1 and neutralizes plant-produced phenolic glycosides. These findings introduce a paradigm by which herbivorous insects can acquire a weapon from their host plants to conversely thwart the plants' chemical defenses, reminiscent of the wisdom of the ancient Chinese philosopher Han Fei, "Attack your shield with your spear." Silencing experiments show that the same wisdom can be applied to combat the global pest.

in total 76 UGTs were identified in the *B. tabaci* MED genome (Guo et al., 2020), we can safely speculate that these whitefly UGTs catalyze the glycosylation of flavonoids with UDP-glucose to generate flavonoid glucosides in *B. tabaci* gut cells as previously reported for *T. urticae* UGTs (Snoeck et al., 2019). Subsequently, these phenolic glucosides can be malonylated in the gut cells by BtPMaT1 via the malonylation reaction as described above. It should be noted that more that 40% of the UGTs do not have a signal peptide (Guo et al., 2020) and are probably cytosolic UGTs that act in concert with BtPMaT1. The flux of malonylated flavonoid glycoside back into the gut lumen might then occur via ATP-binding cassette (ABC) transporters, similar to what has been reported for transport of flavonoids in plants (Zhao, 2015). Overall, our findings reveal that the malonylation of phenolic glycosides catalyzed by BtPMaT1 in gut cells is a key detoxification process in whiteflies.

The evolutionary significance of horizontal gene transfer (HGT) is widely recognized for prokaryotes, but it is now becoming evident that it is also an important driving force for the adaptive evolution of eukaryotes (Husnik and McCutcheon, 2018). Novel traits that evolve through HGT can lead to the exploitation of new resources and niches (Bublitz et al., 2019; Kominek et al., 2019; Soucy et al., 2015; Wang et al., 2020; Wybouw et al., 2016). The donors in HGT events known for arthropods are almost exclusively microorganisms (Wybouw et al., 2016), and empirical evidence for horizontal transfer of functional plant-derived genes to insects has been missing. We show that plant-derived *BtPMaT1* has retained its function and aids *B. tabaci* in coping with ingested phenolic glycosides, present in many of its host plants. Notably, horizontally transferred *BtPMaT1* was detected in different cryptic species of *B. tabaci*, while it was not found in genomes of other insects, including the related greenhouse whitefly, *T. vaporariorum* (Xie et al., 2020). *Bemisia* must have acquired this gene after the divergence from *Trialeurodes* (~86 mya) (Santos-Garcia et al., 2015), and one could hypothesize, that (in addition to other factors) this might explain why *Bemisia* performs better on tomato compared with *Trialeurodes* (Zhang and Wan, 2012).

The HGT of *BtPMaT1* allows the whitefly to use a key element of the plants' arsenal to protect itself from plant defense metabolites (Figure 7). Indeed, tomato also has a phenolic glucoside malonyltransferase (GenBank: XP_025883531, a homolog [68% identity] of NtMaT1 [Taguchi et al., 2005]). This is reminiscent of Han Feizi, a text written during the 3rd century BC by political philosopher Han Fei, in which he famously tells the story of "Attack your shield with your spear." Similar to the gist of this story, we reveal here that whiteflies have adopted their opponent's combat strategy to resist it, and we show that we can apply this same philosophy to control whiteflies. A good understanding of the molecular basis of *B. tabaci*'s polyvalent ability to overcome plant defenses is recognized as a key for the development of durable pest control strategies (Heidel-Fischer and Vogel, 2015). Recent progress has been made. For instance, whiteflies were found to suppress plant defenses by leveraging the crosstalk between plant defense hormones (Zhang et al., 2013), and they may even do so in neighboring plants through the induction of specific volatile signals (Zhang et al., 2019). Several whitefly salivary proteins have been identified as effectors that are involved in this apparent manipulation of plant defenses by eliciting the salicylic acid-signaling pathway (Wang et al., 2019; Xu et al., 2019). Here, we show that whiteflies, in addition to suppressing the synthesis of defensive plant secondary metabolites, also have attained the ability to detoxify defense compounds by acquiring a gene from plants. By silencing *BtPMaT1* in *B. tabaci* adults using different RNAi approaches, we showed that we can disable their immunity to phenolic glycosides. This greatly reduced whitefly performance and offers prospects for whitefly control strategies.

Overall, our findings imply that *B. tabaci* is prone to accept horizontal transfer genes and that this may help to circumvent resistance traits of host plants. This insight into a co-evolutionary process that facilitates host plant adaptation in insects also reveals that interfering with laterally transferred genes can be a highly effective way to combat pests. Indeed, the transgenic expression of dsBtPMaT1 in tomato is lethal to the whiteflies, but does not affect non-target organisms nor does it affect the homologous gene in the host plant because of low nucleic acid

sequence similarity. Mining for other functional horizontal transfer genes from host plants into insect pests should yield other key genes that can be excellent targets for the promising RNAi-based insect pest control strategy.

Limitations of study

This study provides conclusive evidence that the plant-derived gene *BtPMaT1* allows whiteflies to detoxify plant phenolic glucosides, but additional work is needed to fully elucidate its possible other functions. As our phylogenetic analysis showed that BtPMaT1 not only clustered with plant phenolic glucoside malonyltransferases but also with an anthocyanin malonyltransferase, the BtPMaT1 detoxification potential might be broader than we show here. Similarly, we will still need to determine the specific function of the homolog BtPMaT2, which is likely to also contribute to the whitefly's ability to neutralize plant defense metabolites. Also, although we showed that BtPMaT1 and BtPMaT2 were horizontally acquired from plants, we were not able to precisely identify the plant donor species, which might be unveiled when more plant genomes become available.

Transgenic tomatoes expressing the hairpin RNA of *BtPMaT1* gene caused very high whitefly mortality in semi-field experiments, suggesting that these plants may offer an immediate and highly effective solution to control the pest. This remains to be tested under realistic field conditions. The transformation has no apparent effects on the phenotype of young tomato plants, but we will still have to establish possible effects on more mature plants and on tomato yield. Before the transgenic plants can be commercialized, it also still needs to be determined whether the dsRNA produced by the plants affects the performance of other organisms. In this study, we already show that it has no significant effects on aphids or mites.

STAR★METHODS

Detailed methods are provided in the online version of this paper and include the following:

- KEY RESOURCES TABLE
- RESOURCE AVAILABILITY
  - Lead contact
  - Materials availability
  - Data and code availability
- EXPERIMENTAL MODEL AND SUBJECT DETAILS
  - Arthropod strains
- METHOD DETAILS
  - Gut dissection and protein extraction
  - RNA isolation and cDNA synthesis
  - Gene identification and cloning
  - Phylogenetic analysis
  - Bioinformatic analysis
  - gDNA isolation and genome fragment cloning
  - qPCR analysis
  - Metabolite profiling
  - Phenolic glycoside bioassays
  - dsRNA synthesis and RNAi assays
  - VIGS assays
  - Heterologous expression and protein purification
  - Metabolic experiments
  - Honeydew analysis
  - Transgenic experiments
- QUANTIFICATION AND STATISTICAL ANALYSIS

SUPPLEMENTAL INFORMATION

Supplemental information can be found online at https://doi.org/10.1016/j.cell.2021.02.014.

ACKNOWLEDGMENTS

We thank Prof. Xia Cui and Haijing Wang from the Sino-Dutch Joint Laboratory of Horticultural Genomics in our institute for the assistance with the UPLC-QTOF/MS experiment. We also thank all students in our laboratory who helped with dissecting whitefly gut tissues. This research was supported by the National Key R & D Program of China (2019YFD1002100), the National Natural Science Foundation of China (31420103919, 31801747, 32022074), the China Agricultural Research System (CARS-24-C-02), the Beijing Key Laboratory for Pest Control and Sustainable Cultivation of Vegetables, and the Science and Technology Innovation Program of the Chinese Academy of Agricultural Sciences (CAAS-ASTIP-IVFCAAS). The contribution by T.C.J.T. was supported by European Research Council advanced grant 788949.

AUTHOR CONTRIBUTIONS

J.X., Z.G., T.C.J.T., and Y.Z. designed the research. J.X., Z.G., Z.Y., H.H., S.W., H.X., X.Y., F.Y., Q.W., and W.X. performed the experiments. J.X., Z.G., and Z.Y. analyzed the data. J.X., Z.G., X.Z., W.D., T.C.J.T., and Y.Z. wrote and revised the manuscript.

DECLARATION OF INTERESTS

The authors declare that a patent has been filed to the China National Intellectual Property Administration (application no. 202010287105.5).

Received: October 9, 2020
Revised: December 29, 2020
Accepted: February 4, 2021
Published: March 25, 2021

REFERENCES

Ahmad, S., Brattsten, L.B., Mullin, C.A., and Yu, S.J. (1986). Enzymes involved in the metabolism of plant allelochemicals. In Molecular Aspects of Insect-Plant Associations, L.B. Brattsten and S. Ahmad, eds. (Springer US), pp. 73–151.

Berardini, T.Z., Reiser, L., Li, D., Mezheritsky, Y., Muller, R., Strait, E., and Huala, E. (2015). The Arabidopsis information resource: Making and mining the "gold standard" annotated reference plant genome. Genesis *53*, 474–485.

Boeckler, G.A., Gershenzon, J., and Unsicker, S.B. (2011). Phenolic glycosides of the Salicaceae and their role as anti-herbivore defenses. Phytochemistry *72*, 1497–1509.

Bontpart, T., Cheynier, V., Ageorges, A., and Terrier, N. (2015). BAHD or SCPL acyltransferase? What a dilemma for acylation in the world of plant phenolic compounds. New Phytol. *208*, 695–707.

Bublitz, D.C., Chadwick, G.L., Magyar, J.S., Sandoz, K.M., Brooks, D.M., Mesnage, S., Ladinsky, M.S., Garber, A.I., Bjorkman, P.J., Orphan, V.J., and McCutcheon, J.P. (2019). Peptidoglycan production by an insect-bacterial mosaic. Cell *179*, 703–712.e7.

Chen, W., Hasegawa, D.K., Kaur, N., Kliot, A., Pinheiro, P.V., Luan, J., Stensmyr, M.C., Zheng, Y., Liu, W., Sun, H., et al. (2016). The draft genome of whitefly *Bemisia tabaci* MEAM1, a global crop pest, provides novel insights

into virus transmission, host adaptation, and insecticide resistance. BMC Biol. *14*, 110.

Chu, D., Wan, F.H., Zhang, Y.J., and Brown, J.K. (2010). Change in the biotype composition of *Bemisia tabaci* in Shandong Province of China from 2005 to 2008. Environ. Entomol. *39*, 1028–1036.

D'Auria, J.C. (2006). Acyltransferases in plants: a good time to be BAHD. Curr. Opin. Plant Biol. *9*, 331–340.

De Barro, P.J., Liu, S.S., Boykin, L.M., and Dinsdale, A.B. (2011). *Bemisia tabaci*: a statement of species status. Annu. Rev. Entomol. *56*, 1–19.

Després, L., David, J.P., and Gallet, C. (2007). The evolutionary ecology of insect resistance to plant chemicals. Trends Ecol. Evol. *22*, 298–307.

Erb, M., and Reymond, P. (2019). Molecular interactions between plants and insect herbivores. Annu. Rev. Plant Biol. *70*, 527–557.

Frear, D.S., Mansager, E.R., Swanson, H.R., and Tanaka, F.S. (1983). Metribuzin metabolism in tomato: Isolation and identification of N-glucoside conjugates. Pestic. Biochem. Physiol. *19*, 270–281.

Gilbertson, R.L., Batuman, O., Webster, C.G., and Adkins, S. (2015). Role of the insect supervectors *Bemisia tabaci* and *Frankliniella occidentalis* in the emergence and global spread of plant viruses. Annu. Rev. Virol. *2*, 67–93.

Guo, L., Xie, W., Yang, Z., Xu, J., and Zhang, Y. (2020). Genome-wide identification and expression analysis of UDP-glucuronosyltransferases in the whitefly *Bemisia tabaci* (Gennadius) (Hemiptera: Aleyrodidae). Int. J. Mol. Sci. *21*, 8492.

Heidel-Fischer, H.M., and Vogel, H. (2015). Molecular mechanisms of insect adaptation to plant secondary compounds. Curr. Opin. Insect Sci. *8*, 8–14.

Higuchi, Y., and Kawakita, A. (2019). Leaf shape deters plant processing by an herbivorous weevil. Nat. Plants *5*, 959–964.

Husnik, F., and McCutcheon, J.P. (2018). Functional horizontal gene transfer from bacteria to eukaryotes. Nat. Rev. Microbiol. *16*, 67–79.

Jones, P., Binns, D., Chang, H.Y., Fraser, M., Li, W., McAnulla, C., McWilliam, H., Maslen, J., Mitchell, A., Nuka, G., et al. (2014). InterProScan 5: genome-scale protein function classification. Bioinformatics *30*, 1236–1240.

Katoh, K., and Standley, D.M. (2013). MAFFT multiple sequence alignment software version 7: improvements in performance and usability. Mol. Biol. Evol. *30*, 772–780.

Kominek, J., Doering, D.T., Opulente, D.A., Shen, X.X., Zhou, X., DeVirgilio, J., Hulfachor, A.B., Groenewald, M., Mcgee, M.A., Karlen, S.D., et al. (2019). Eukaryotic acquisition of a bacterial operon. Cell *176*, 1356–1366.e10.

Kumar, S., Stecher, G., and Tamura, K. (2016). MEGA7: molecular evolutionary genetics analysis version 7.0 for bigger datasets. Mol. Biol. Evol. *33*, 1870–1874.

Lao, S.H., Loutre, C., Brazier, M., Coleman, J.O.D., Cole, D.J., Edwards, R., and Theodoulou, F.L. (2003). 3,4-Dichloroaniline is detoxified and exported via different pathways in *Arabidopsis* and soybean. Phytochemistry *63*, 653–661.

Lattanzio, V., Lattanzio, V.M.T., and Cardinali, A. (2006). Role of phenolics in the resistance mechanisms of plants against fungal pathogens and insects. In Phytochemistry: Advances In Research, F. Imperato, ed. (Research Signpost), pp. 23–67.

Leiss, K.A., Choi, Y.H., Abdel-Farid, I.B., Verpoorte, R., and Klinkhamer, P.G. (2009). NMR metabolomics of thrips (*Frankliniella occidentalis*) resistance in *Senecio* hybrids. J. Chem. Ecol. *35*, 219–229.

Li, W., and Godzik, A. (2006). Cd-hit: a fast program for clustering and comparing large sets of protein or nucleotide sequences. Bioinformatics *22*, 1658–1659.

Li, R., Xie, W., Wang, S., Wu, Q., Yang, N., Yang, X., Pan, H., Zhou, X., Bai, L., Xu, B., et al. (2013). Reference gene selection for qRT-PCR analysis in the sweetpotato whitefly, *Bemisia tabaci* (Hemiptera: Aleyrodidae). PLoS ONE *8*, e53006.

Lindroth, R.L. (1988). Hydrolysis of phenolic glycosides by midgut β-glucosidases in *Papilio glaucus* subspecies. Insect Biochem. *18*, 789–792.

Liu, Y., Schiff, M., and Dinesh-Kumar, S.P. (2002). Virus-induced gene silencing in tomato. Plant J. *31*, 777–786.

Liu, S.S., De Barro, P.J., Xu, J., Luan, J.B., Zang, L.S., Ruan, Y.M., and Wan, F.H. (2007). Asymmetric mating interactions drive widespread invasion and displacement in a whitefly. Science *318*, 1769–1772.

Livak, K.J., and Schmittgen, T.D. (2001). Analysis of relative gene expression data using real-time quantitative PCR and the $2^{(-\Delta\ \Delta\ C(T))}$ Method. Methods *25*, 402–408.

Malka, O., Easson, M.L.A.E., Paetz, C., Götz, M., Reichelt, M., Stein, B., Luck, K., Stanišić, A., Juravel, K., Santos-Garcia, D., et al. (2020). Glucosylation prevents plant defense activation in phloem-feeding insects. Nat. Chem. Biol. *16*, 1420–1426.

Mierziak, J., Kostyn, K., and Kulma, A. (2014). Flavonoids as important molecules of plant interactions with the environment. Molecules *19*, 16240–16265.

Miller, M.A., Pfeiffer, W., and Schwartz, T. (2012). The CIPRES science gateway: enabling high-impact science for phylogenetics researchers with limited resources. In Proceedings of the 1st Conference of the Extreme Science and Engineering Discovery Environment: Bridging from the eXtreme to the campus and beyond, E. Stewart, ed. (Association for Computing Machinery), pp. 1–8.

Mithöfer, A., and Boland, W. (2012). Plant defense against herbivores: chemical aspects. Annu. Rev. Plant Biol. *63*, 431–450.

Nilsson, O., Little, C.H., Sandberg, G., and Olsson, O. (1996). Expression of two heterologous promoters, *Agrobacterium rhizogenes rolC* and cauliflower mosaic virus *35S*, in the stem of transgenic hybrid aspen plants during the annual cycle of growth and dormancy. Plant Mol. Biol. *31*, 887–895.

Oliveira, M.R.V., Henneberry, T.J., and Anderson, P. (2001). History, current status, and collaborative research projects for *Bemisia tabaci*. Crop Prot. *20*, 709–723.

Onkokesung, N., Reichelt, M., van Doorn, A., Schuurink, R.C., van Loon, J.J., and Dicke, M. (2014). Modulation of flavonoid metabolites in *Arabidopsis thaliana* through overexpression of the *MYB75* transcription factor: role of kaempferol-3,7-dirhamnoside in resistance to the specialist insect herbivore *Pieris brassicae*. J. Exp. Bot. *65*, 2203–2217.

Opitz, S.E.W., and Müller, C. (2009). Plant chemistry and insect sequestration. Chemoecology *19*, 117–154.

Park, S.H., Morris, J.L., Park, J.E., Hirschi, K.D., and Smith, R.H. (2003). Efficient and genotype-independent *Agrobacterium*–mediated tomato transformation. J. Plant Physiol. *160*, 1253–1257.

Price, P.W., Denno, R.F., Eubanks, M.D., Finke, D.L., and Kaplan, I. (2011). Insect Ecology: Behavior, Populations and Communities (New York: Cambridge University Press).

Santos-Garcia, D., Vargas-Chavez, C., Moya, A., Latorre, A., and Silva, F.J. (2015). Genome evolution in the primary endosymbiont of whiteflies sheds light on their divergence. Genome Biol. Evol. *7*, 873–888.

Snoeck, S., Pavlidi, N., Pipini, D., Vontas, J., Dermauw, W., and Van Leeuwen, T. (2019). Substrate specificity and promiscuity of horizontally transferred UDP-glycosyltransferases in the generalist herbivore *Tetranychus urticae*. Insect Biochem. Mol. Biol. *109*, 116–127.

Soucy, S.M., Huang, J., and Gogarten, J.P. (2015). Horizontal gene transfer: building the web of life. Nat. Rev. Genet. *16*, 472–482.

Speed, M.P., Fenton, A., Jones, M.G., Ruxton, G.D., and Brockhurst, M.A. (2015). Coevolution can explain defensive secondary metabolite diversity in plants. New Phytol. *208*, 1251–1263.

Stamatakis, A. (2014). RAxML version 8: a tool for phylogenetic analysis and post-analysis of large phylogenies. Bioinformatics *30*, 1312–1313.

Su, Q., Mescher, M.C., Wang, S., Chen, G., Xie, W., Wu, Q., Wang, W., and Zhang, Y. (2016). Tomato yellow leaf curl virus differentially influences plant defence responses to a vector and a non-vector herbivore. Plant Cell Environ. *39*, 597–607.

Suzuki, H., Nakayama, T., Yonekura-Sakakibara, K., Fukui, Y., Nakamura, N., Yamaguchi, M.A., Tanaka, Y., Kusumi, T., and Nishino, T. (2002). cDNA cloning, heterologous expressions, and functional characterization of malonyl-

coenzyme a:anthocyanidin 3-*o*-glucoside-6"-*o*-malonyltransferase from dahlia flowers. Plant Physiol. *130*, 2142–2151.

Taguchi, G., Shitchi, Y., Shirasawa, S., Yamamoto, H., and Hayashida, N. (2005). Molecular cloning, characterization, and downregulation of an acyltransferase that catalyzes the malonylation of flavonoid and naphthol glucosides in tobacco cells. Plant J. *42*, 481–491.

Taguchi, G., Ubukata, T., Nozue, H., Kobayashi, Y., Takahi, M., Yamamoto, H., and Hayashida, N. (2010). Malonylation is a key reaction in the metabolism of xenobiotic phenolic glucosides in *Arabidopsis* and tobacco. Plant J. *63*, 1031–1041.

Terahara, N. (2015). Flavonoids in foods: a review. Nat. Prod. Commun. *10*, 521–528.

Tian, L., Song, T., He, R., Zeng, Y., Xie, W., Wu, Q., Wang, S., Zhou, X., and Zhang, Y. (2017). Genome-wide analysis of ATP-binding cassette (ABC) transporters in the sweetpotato whitefly, *Bemisia tabaci*. BMC Genomics *18*, 330.

Tuominen, L.K., Johnson, V.E., and Tsai, C.J. (2011). Differential phylogenetic expansions in BAHD acyltransferases across five angiosperm taxa and evidence of divergent expression among *Populus paralogues*. BMC Genomics *12*, 236.

Van Leeuwen, T., Demaeght, P., Osborne, E.J., Dermauw, W., Gohlke, S., Nauen, R., Grbić, M., Tirry, L., Merzendorfer, H., and Clark, R.M. (2012). Population bulk segregant mapping uncovers resistance mutations and the mode of action of a chitin synthesis inhibitor in arthropods. Proc. Natl. Acad. Sci. USA *109*, 4407–4412.

Vandesompele, J., De Preter, K., Pattyn, F., Poppe, B., Van Roy, N., De Paepe, A., and Speleman, F. (2002). Accurate normalization of real-time quantitative RT-PCR data by geometric averaging of multiple internal control genes. Genome Biol. *3*, H0034.

Walle, T. (2004). Absorption and metabolism of flavonoids. Free Radic. Biol. Med. *36*, 829–837.

Wang, N., Zhao, P., Ma, Y., Yao, X., Sun, Y., Huang, X., Jin, J., Zhang, Y., Zhu, C., Fang, R., and Ye, J. (2019). A whitefly effector Bsp9 targets host immunity regulator WRKY33 to promote performance. Philos. Trans. R. Soc. Lond. B Biol. Sci. *374*, 20180313.

Wang, H., Sun, S., Ge, W., Zhao, L., Hou, B., Wang, K., Lyu, Z., Chen, L., Xu, S., Guo, J., et al. (2020). Horizontal gene transfer of *Fhb7* from fungus underlies *Fusarium* head blight resistance in wheat. Science *368*, eaba5435.

Wybouw, N., Pauchet, Y., Heckel, D.G., and Van Leeuwen, T. (2016). Horizontal gene transfer contributes to the evolution of arthropod herbivory. Genome Biol. Evol. *8*, 1785–1801.

Xie, W., Chen, C., Yang, Z., Guo, L., Yang, X., Wang, D., Chen, M., Huang, J., Wen, Y., Zeng, Y., et al. (2017). Genome sequencing of the sweetpotato whitefly *Bemisia tabaci* MED/Q. Gigascience *6*, 1–7.

Xie, W., He, C., Fei, Z., and Zhang, Y. (2020). Chromosome-level genome assembly of the greenhouse whitefly (*Trialeurodes vaporariorum* Westwood). Mol. Ecol. Resour. *20*, 995–1006.

Xiong, Y., Zeng, H., Zhang, Y., Xu, D., and Qiu, D. (2013). Silencing the *HaHR3* gene by transgenic plant-mediated RNAi to disrupt *Helicoverpa armigera* development. Int. J. Biol. Sci. *9*, 370–381.

Xu, H.X., Qian, L.X., Wang, X.W., Shao, R.X., Hong, Y., Liu, S.S., and Wang, X.W. (2019). A salivary effector enables whitefly to feed on host plants by eliciting salicylic acid-signaling pathway. Proc. Natl. Acad. Sci. USA *116*, 490–495.

Yu, X.H., Gou, J.Y., and Liu, C.J. (2009). BAHD superfamily of acyl-CoA dependent acyltransferases in *Populus* and *Arabidopsis*: bioinformatics and gene expression. Plant Mol. Biol. *70*, 421–442.

Zhang, G.F., and Wan, F.H. (2012). Suitability changes with host leaf age for *Bemisia tabaci* B biotype and *Trialeurodes vaporariorum*. Environ. Entomol. *41*, 1125–1130.

Zhang, P.J., Broekgaarden, C., Zheng, S.J., Snoeren, T.A., van Loon, J.J., Gols, R., and Dicke, M. (2013). Jasmonate and ethylene signaling mediate whitefly-induced interference with indirect plant defense in *Arabidopsis thaliana*. New Phytol. *197*, 1291–1299.

Zhang, P.J., Wei, J.N., Zhao, C., Zhang, Y.F., Li, C.Y., Liu, S.S., Dicke, M., Yu, X.P., and Turlings, T.C.J. (2019). Airborne host-plant manipulation by whiteflies via an inducible blend of plant volatiles. Proc. Natl. Acad. Sci. USA *116*, 7387–7396.

Zhao, J. (2015). Flavonoid transport mechanisms: how to go, and with whom. Trends Plant Sci. *20*, 576–585.

Zhao, J., Huhman, D., Shadle, G., He, X.Z., Sumner, L.W., Tang, Y., and Dixon, R.A. (2011). MATE2 mediates vacuolar sequestration of flavonoid glycosides and glycoside malonates in *Medicago truncatula*. Plant Cell *23*, 1536–1555.

STAR★METHODS

KEY RESOURCES TABLE

REAGENT or RESOURCE	SOURCE	IDENTIFIER
Antibodies		
Anti-His(C-term)-HRP Antibody	Thermo Fisher Scientific	Cat# R931-25; RRID: AB_2556554
Goat anti-Mouse IgG H&L (HRP) secondary antibody	Abcam	Cat# ab7068; RRID: AB_955413
Bacterial and virus strains		
Agrobacterium tumefaciens GV3101	This study	N/A
Agrobacterium tumefaciens LBA4404	This study	N/A
Biological samples		
DNA of whitefly and tomato samples	This study	N/A
RNA of whitefly and tomato samples	This study	N/A
Protein of whitefly gut tissues	This study	N/A
Whitefly honeydew and tomato leaves for metabolic profiling	This study	N/A
Chemicals, peptides, and recombinant proteins		
Phenyl β-D-glucoside	Yuanye Biotech	Cat# S24698
4-nitrophenyl β-D-glucoside	Yuanye Biotech	Cat# S10138
Salicin	MEC	Cat# HY-N0149
Androsin	MREDA	Cat# M043612
Verbascoside	MEC	Cat# HY-N0021
4-methylumbelliferone glucoside	Yuanye Biotech	Cat# S11118
Polygalaxanthone III	Solarbio	Cat# SP8440
Rhaponticin	MREDA	Cat# M044379
Kaempferol 7-O-glucoside	Yuanye Biotech	Cat# B21130
Kaempferol 3-O-glucoside	Yuanye Biotech	Cat# B21704
Phlorizin	Yuanye Biotech	Cat# B20449
Malonyl-CoA	Sigma-Aldrich	Cat# M4263
Kaempferol 3-O-(6-malonyl-glucoside)	BOC Sciences	Cat# 81149-02-2
Quercetin 3-O-β-D-glucoside	Meilunbio	Cat# MB7017
Apigenin-7-O-glucoside	Psaitong	Cat# A10718
Naringenin-7-O-glucoside	Psaitong	Cat# N10139
Peonidin-3-glucoside	Sigma-Aldrich	Cat# 40796
Acetonitrile	Thermo Fisher Scientific	Cat# A955-4
Methanol	Thermo Fisher Scientific	Cat# A456-4
Formic acid	Thermo Fisher Scientific	Cat# A117-50
*Xba*I	NEB	Cat# R0145V
*Sac*I	NEB	Cat# R3156V
BamHI	NEB	Cat# R0136V
HindIII	NEB	Cat# R0104V
*Xho*I	NEB	Cat# R0146M
BglII	NEB	Cat# R0144L
T4 DNA Ligase	NEB	Cat# M0202L
Protease inhibitor cocktail (Complete tablets EDTA-free, EASYpack)	Roche	Cat# 4693132001
DIG-11-UTP	Roche	Cat# 03359247910

(*Continued on next page*)

Continued

REAGENT or RESOURCE	SOURCE	IDENTIFIER
Critical commercial assays		
SuperSignal West Pico Chemiluminescent Substrate	Thermo Fisher Scientific	Cat# 34577
PrimeScript II 1st strand cDNA synthesis kit	TaKaRa	Cat# 6210B
PrimeScript RT kit	TaKaRa	Cat# RR014A
pEASY-T1 vector	TransGen	Cat# CT101-01
Trans1-T1 competent cells	TransGen	Cat# CD501-02
TIANamp Blood/Tissue/Cell Genomic DNA Extraction Kit DP304	TIANGEN	Cat# DP304-02
SuperReal PreMix Plus (SYBR Green)	TIANGEN	Cat# FP205-01
50 × ROX Reference Dye	TIANGEN	Cat# FP205-01
T7 Ribomax Express RNAi System	Promega	Cat# P1700
Bac-to-Bac Baculovirus Expression System	Invitrogen	Cat# 10359016
Cellfectin II Reagent	Invitrogen	Cat# 10362100
Sf-900 II SFM	Thermo Fisher Scientific	Cat# 21012026
HisTrap HP 5 ml column	GE Healthcare	Cat# 17524802
HiTrap desalting 5 ml column	GE Healthcare	Cat# 17140801
Plant Genomic DNA Kit	TIANGEN	Cat# DP305-02
Deposited data		
Bemisia tabaci MED genome	Xie et al., 2017	http://gigadb.org/dataset/100286
RNA-seq data for *Bemisia tabaci* MED	Tian et al., 2017	NCBI SRA: SRP064690
Bemisia tabaci MEAM1 genome	Chen et al., 2016	http://www.whiteflygenomics.org/cgi-bin/bta/index.cgi
Trialeurodes vaporariorum genome	Xie et al., 2020	https://www.ncbi.nlm.nih.gov/assembly/GCA_011764245.1
The *BtPMaT1* gene of *B. tabaci* MED	This study	NCBI GenBank: MN756010
The *BtPMaT1* gene of *B. tabaci* New World	This study	NCBI GenBank: MW387250
The *BtPMaT1* gene of *B. tabaci* Asia II 3	This study	NCBI GenBank: MW387251
Experimental models: cell lines		
Spodoptera frugiperda: cell line Sf9	Invitrogen	Cat# B82501
Experimental models: organisms/strains		
B. tabaci MED reared on poinsettia (*Euphorbia pulcherrima* Wild. ex Kl.)	This study	N/A
B. tabaci MED reared on cotton (*Gossypium herbaceum* L. cv. DP99B)	This study	N/A
B. tabaci MED reared on tomato (*Solanum lycopersicum* Miller, cv. Zhongza 9)	This study	N/A
Myzus persicae reared on tomato (*Solanum lycopersicum* Miller, cv. Zhongza 9)	This study	N/A
Tetranychus urticae reared on tomato (*Solanum lycopersicum* Miller, cv. Zhongza 9)	This study	N/A
Tomato (*Solanum lycopersicum* Miller, cv. Zhongza 9)	This study	N/A
Tomato (*Solanum lycopersicum* cv. Moneymaker)	This study	N/A
Oligonucleotides		
Primers for *BtPMaT1* gene cloning, see Table S1	This study	N/A
Primers for genome fragment cloning, see Table S1	This study	N/A
Primers for RT-qPCR, see Table S1	This study	N/A
Primers for RNAi, see Table S1	This study	N/A

(*Continued on next page*)

Continued		
REAGENT or RESOURCE	SOURCE	IDENTIFIER
Primers for VIGS, see Table S1	This study	N/A
Primers for *BtPMaT1* heterologous expression, see Table S1	This study	N/A
Primers for transgenic detection, see Table S1	This study	N/A
Recombinant DNA		
VIGS (pTRV1 and pTRV2)	Liu et al., 2002	N/A
pTRV2-BtPMaT1	This study	N/A
pTRV2-EGFP	This study	N/A
pRNAi1017 and PCAMBIA2300-35S-OCS	Xiong et al., 2013	N/A
pRNAi-BtPMaT1	This study	N/A
pCAMBIA-RNAi-BtPMaT1	This study	N/A
Software and algorithms		
InterProScan	Jones et al., 2014	https://www.ebi.ac.uk/interpro/
CD-HIT	Li and Godzik, 2006	http://weizhongli-lab.org/cd-hit/
MAFFT version 7	Katoh and Standley, 2013	https://mafft.cbrc.jp/alignment/software/
CIPRES Science Gateway	Miller et al., 2012	http://www.phylo.org/
RaXML-HPC2 version 8.2.12	Stamatakis, 2014	https://github.com/stamatak/standard-RAxML
MEGA7	Kumar et al., 2016	https://www.megasoftware.net
Primer Premier 5.0	Premier Biosoft	http://www.premierbiosoft.com/primerdesign/
Progenesis QI	Waters	https://www.waters.com/waters/en_US/Progenesis-QI/nav.htm?cid=134790652&lset=1&locale=en_US&changedCountry=Y
UNIFI	Waters	https://www.waters.com/waters/en_US/Natural-Products-Application-Solution-with-UNIFI/nav.htm?cid=134777097&lset=1&locale=en_US&changedCountry=Y
IGV 2.3	Broad Institute and the Regents of the University of California	http://software.broadinstitute.org/software/igv/
SnapDragon	Harvard Medical College	https://www.flyrnai.org/cgi-bin/RNAi_find_primers.pl
GraphPad Prism 8	GraphPad Software	https://www.graphpad.com/
SigmaPlot 14.0	Systat Software, Inc	https://systatsoftware.com/products/sigmaplot/
SPSS V23.0	IBM	https://www.ibm.com/analytics/spss-statistics-software

RESOURCE AVAILABILITY

Lead contact

Further information and requests for resources and reagents should be directed to and will be fulfilled by the Lead Contact, Youjun Zhang (zhangyoujun@caas.cn).

Materials availability

The study did not generate new unique reagents.

Data and code availability

The full-length cDNA sequences of *BtPMaT1* in *B. tabaci* MED, New World and Asia II 3 cryptic species of this study have been deposited in GenBank with the accession numbers MN756010, MW387250 and MW387251.

EXPERIMENTAL MODEL AND SUBJECT DETAILS

Arthropod strains

A strain of *B. tabaci* MED that was originally collected in 2009 from poinsettia (*Euphorbia pulcherrima* Wild. ex Kl.) in Beijing, was subsequently maintained on poinsettia and cotton plants (*Gossypium herbaceum* L. cv. DP99B) to establish a poinsettia strain and a cotton strain, respectively. A pepper strain that originated from *B. tabaci* MED collected from cucumber plants in Beijing in 2011, was subsequently transferred to caged pepper plants as previously described (Xie et al., 2017). A tomato strain of *B. tabaci* MED was collected in 2018 from tomato plants in Beijing and was subsequently reared on tomato (*Solanum lycopersicum* Miller, cv. Zhongza 9). The purity of each of these four strains was monitored by sequencing a fragment of the mitochondrial cytochrome oxidase I (mtCOI) gene every three to five generations (Chu et al., 2010). All of the *B. tabaci* strains were maintained in a glasshouse at 27 ± 1°C, 60%–80% relative humidity (RH), and a photoperiod of L16:D8. In this study, all four *B. tabaci* MED host plant strains were used to detect the presence of the *BtPMaT1* gene while in all the other experiments only the cotton strain was used.

The aphid *Myzus persicae* used in this study was originally collected from pakchoi in 2017 at Ningde, Fujian Province, China. Subsequently, this *M. persicae* population was maintained in the laboratory on radish seedling. A subset of this strain was transferred and continuously reared on tomato (*Solanum lycopersicum* Miller, cv. Zhongza 9) for more than one year at 26 ± 2°C, with a 60%–80% RH and a photoperiod of L16:D8, and was used in our experiments.

The two-spotted spider mite *T. urticae* used in this study was originally collected from an apple orchard in 2009 at Tai'an, Shandong Province, China (Su et al., 2016). Subsequently, this *T. urticae* population was maintained in the laboratory on detached bean leaves (*Phaseolus vulgaris* L. cv. Bifeng). A subset of this strain has been continuously reared on tomato (*Solanum lycopersicum* Miller, cv. Zhongza 9) for more than one year at 26 ± 2°C, with a 60%–80% RH and a photoperiod of L16:D8, and was used in our experiments.

METHOD DETAILS

Gut dissection and protein extraction

Gut tissues of *B. tabaci* MED adults (Figure S5D) were carefully dissected in ice-cold phosphate-buffered saline (PBS) buffer (pH 7.4) (Sigma-Aldrich). For qPCR analyses, gut tissues and the rest of the body (non-gut body) from about 1000 adults were collected in triplicate and stored in TRIzol reagent (Invitrogen) at −80°C until further use. For malonyltransferase activity measurements, gut tissues were dissected from approximately 10000 adults in PBS buffer containing a protease inhibitor cocktail (Complete tablets EDTA-free, EASYpack, Roche). The obtained gut tissues were pooled, homogenized and ultrasonically disrupted on ice for 6 min. After centrifugation at 12000 × *g* at 4°C for 10 min, the soluble gut proteins in the supernatant were collected and quantified using the NanoDrop 2000c spectrophotometer (Thermo Fisher Scientific), flash frozen and kept at −80°C until further use.

RNA isolation and cDNA synthesis

Total RNA was extracted from *B. tabaci* MED samples using TRIzol reagent (Invitrogen) according to the manufacturer's recommendations. Agarose gel electrophoresis was used to determine the integrity of the RNA, and a NanoDrop 2000c spectrophotometer (Thermo Fisher Scientific) was used to quantify the RNA. cDNA was synthesized using the PrimeScript II 1st strand cDNA synthesis kit (TaKaRa) and PrimeScript RT kit (containing gDNA Eraser, Perfect Real Time) (TaKaRa) for *BtPMaT1* gene cloning and qPCR analysis, respectively. The synthesized cDNA was immediately stored at −20°C until used.

Gene identification and cloning

The *BtPMaT1* gene was found in our recently sequenced *B. tabaci* MED genome (Gene ID: BTA023005.1, http://gigadb.org/dataset/100286) (Xie et al., 2017) and annotated as a phenolic glucoside malonyltransferase. For the cloning of *BtPMaT1*, the putative CDS of *BtPMaT1* was manually corrected using our previous completed transcriptome data of *B. tabaci* MED (Tian et al., 2017). Specific primers used for gene cloning (Table S1) were designed using Primer Premier 5.0, and the PCR amplicon from the *B. tabaci* MED was cloned into the pEASY-T1 (TransGen) vector and transformed into *Escherichia coli* Trans1-T1 competent cells (TransGen) for sequencing. The full-length cDNA sequence of *BtPMaT1* was deposited in the GenBank database (accession number MN756010).

Phylogenetic analysis

The BtPMaT1 protein sequence was used as a query in a tBLASTn and BLASTp search (with "Expect threshold" set at 1E-15) against the *B. tabaci* MED (http://gigadb.org/dataset/100286) and MEAM1 (http://www.whiteflygenomics.org/cgi-bin/bta/index.cgi) genomes and their predicted protein datasets, respectively (Chen et al., 2016; Xie et al., 2017). BtPMaT1 and BTA005164.2 (BtPMaT2) were subsequently used in a BLASTp and tBLASTn search (with "Expect threshold" set at 1E-15) against the NCBI-non-redundant protein and nucleotide database (version of December 2020), with the "Organism" tab set to "Arthropoda." Next, BtPMaT1 and BtPMaT2 were used as a query in an unrestricted BLASTp search (with "Expect threshold" set at 1E-15) against the NCBI non-redundant protein database. The top ten hits, together with a random selection of 9-10 hits with a gradually increasing E-value (E-value interval of E-10), were downloaded for each BLASTp search. BtPMaT1 and BtPMaT2 were also used in a BLASTp search against the NCBI non-redundant protein database, with Viridiplantae and *B. tabaci* excluded in the "Organism" tab and the top ten BLASTp

hits with a sequence length of more than 400 amino acids (aa) were retrieved. Last, BtPMaT1 and BtPMaT2 were used in a BLASTp search against the model plant *A. thaliana* at the TAIR database (Berardini et al., 2015) and the resulting hits (> 400 aa in length, E-value < E-15) were merged with those collected as described above, a set of previously characterized plant malonyltransferases [GmIMaT3, GmMaT4, MtMaT4 Ss5MaT1, Vh3MaT1, Lp3MaT1 and NtMaT1 (Bontpart et al., 2015)] and two basal members of the BAHD superfamily of acyltransferases [*A. thaliana* CER2, and *Zea mays* Glossy2 (Tuominen et al., 2011; Yu et al., 2009)]. This set of sequences was subsequently filtered for highly similar protein sequences using CD-HIT with the "-c 0.95" option (Li and Godzik, 2006), resulting in a final dataset of 75 sequences. This filtered protein set was then aligned using the online version of MAFFT version 7 with G-INSI-i settings (Katoh and Standley, 2013) (see Data S1) and a maximum likelihood analysis was performed on the CIPRES Science Gateway (Miller et al., 2012) using RaXML-HPC2 version 8.2.12 on XSEDE (Stamatakis, 2014), with 1000 rapid bootstraps and protein model set to "auto" (RaXML options set to "-p 12345 -m PROTGAMMAAUTO -f a -N 1000 -x 12345"). The resulting tree was midpoint rooted and tree layout was further edited using MEGA7 (Kumar et al., 2016).

Bioinformatic analysis

Illumina DNA reads that were generated during sequencing of the genome of *B. tabaci* MED, *B. tabaci* MEAM1, *B. tabaci* Asia II 3 and *B. tabaci* New World cryptic species and Illumina RNA-seq reads from *B. tabaci* MED adult polyA-selected RNA (Tian et al., 2017) were mapped as previously described (Van Leeuwen et al., 2012). The read alignments and coverage were visualized by the IGV 2.3 software (http://software.broadinstitute.org/software/igv/). The genome fragments surrounding *BtPMaT1* of *B. tabaci* MED (http://gigadb.org/dataset/100286) and *B. tabaci* MEAM1 (http://www.whiteflygenomics.org/cgi-bin/bta/index.cgi) were analyzed as described before (Chen et al., 2016; Xie et al., 2017), while any possible synteny between the *B. tabaci* genomic region that contains *BtPMaT1* (and its neighboring serine protease genes) and the *T. vaporarorium* genome (https://www.ncbi.nlm.nih.gov/assembly/GCA_011764245.1) (Xie et al., 2020) was investigated using a BLAST approach.

gDNA isolation and genome fragment cloning

Genomic DNA (gDNA) was extracted from *B. tabaci* MED adults using the TIANamp Blood/Tissue/Cell Genomic DNA Extraction Kit DP304 (TIANGEN) following the manufacturer's recommendations. For target genome fragment cloning, specific primers to amplify the genome region between the *BtPMaT1* and neighboring genes were designed using Primer Premier 5.0 (Table S1). Genome fragments obtained by PCR amplification were ligated into the pEASY-T1 vector (TransGen) and subsequently transformed into Trans1-T1 competent cells (TransGen) for sequencing.

qPCR analysis

The gene-specific primers of *BtPMaT1* used for the real time-quantitative PCR (qPCR) analysis were designed by Primer Premier 5.0 (Table S1). The 25 μL PCR reactions included 0.5 μL of 50 × ROX Reference Dye (TIANGEN), 0.75 μL of each specific primer, 1 μL of cDNA template, 9.5 μL of ddH_2O, and 12.5 μL of 2 × SuperReal PreMix Plus (SYBR Green) (TIANGEN). The qPCR reactions were performed in an ABI 7500 system (Applied Biosystems) with the following protocol: initial denaturation of 94°C for 3 min, followed by 40 cycles of 95°C for 15 s, 60°C for 30 s, and 72°C for 30 s. The amplification efficiencies were determined by dissociation curve analysis using five 2-fold serial dilutions of *B. tabaci* cDNA template. Only primers with 90%–110% amplification efficiencies were used for the subsequent studies.

Relative quantification was calculated according to the $2^{-\Delta\Delta Ct}$ method (Livak and Schmittgen, 2001), to accurately analyze the expressions of the target gene, the expression data were normalized to the geometric mean of internal genes including elongation factor 1 alpha (*EF1-α*) (GenBank accession number EE600682) and 60S ribosomal protein L29 (*RPL29*) (GenBank accession number EE596314) (Li et al., 2013; Vandesompele et al., 2002). Three independent biological replicates and four technical replicates were performed for each whitefly sample.

Metabolite profiling

Each fresh sample (tomato leaves) was immediately frozen with liquid nitrogen and ground into powder. 500 mg tomato leaf powder was extracted with 4 mL methanol/formic acid (HPLC grade, Thermo Fisher Scientific) (9:1 v/v) in 50 mL centrifugal tube at 4°C for 12 h. After centrifugation at 5000 × *g* for 20 min, 2 mL supernatant was dried up under nitrogen gas flow. The dried extract was dissolved in 1 mL methanol/formic acid (9:1, v/v), then filtered through a 0.22 μm nylon membrane. The extract was stored at −20°C until used. Three biological replicates were performed for each sample.

An ultra-performance liquid chromatography/quadrupole time-of-flight mass spectrometer (UPLC-QTOF/MS) system (Waters) was used for the identification of widely targeted metabolites in dried tomato leaves samples. The ChemSpider library including the MS and MS/MS spectra was established by the untargeted method based on the total scan ESI (ESI-QTOF-MS/MS). Full time-of-flight (TOF) scans were acquired in the mass range of *m/z* 100-1500 at positive acquisition mode using the ACQUITY UPLC I-Class/Xevo G2-XS QTOF system (Waters). The acquisition time of mass was 60 min in total, and scan time was 1.5 scan per second. The solvent A and solvent B for UPLC were acetonitrile (HPLC grade, Thermo Fisher Scientific) with 5% formic acid and water with 5% formic acid, respectively. The UPLC was conducted with 60 min run time and 0.15 ml/min flow rate. Solvent A started at 2.5%, ramped to 10% in 5 min, and ramped from 5 to 20 min at 25%. Then solvent A was kept at 25% from 20 min to 25 min, and changed back to 2.5% from 25 min to 60 min. Column temperature and sample room temperature were set at 25°C

and 20°C, respectively. The injection needle was rinsed for 3 s before and after injection. The PDA detector was set to scan the range from 190 to 800 nm, and sampling rate was 20 points per second. The commercial metabolites database Progenesis QI (Waters) was used to analyze the mass data. The phenolic glucosides were manually filtered from the identified compounds. Results are shown in Figure 2 and Table S2.

Phenolic glycoside bioassays

Newly emerged adults (0- to 2-day-old) of *B. tabaci* MED were fed with diet containing one of the following 11 phenolic glycosides in feeding chambers (Figure 3A): phenyl β-D-glucoside (Yuanye Biotech, ≥ 98%), 4-nitrophenyl β-D-glucoside (Yuanye Biotech, ≥ 98%), salicin (MEC, ≥ 98%), androsin (MREDA, ≥ 98%), verbascoside (MEC, ≥ 98%), 4-methylumbelliferone glucoside (Yuanye Biotech, ≥ 99%), polygalaxanthone III (Solarbio, ≥ 98%), rhaponticin (MREDA, ≥ 98%), kaempferol 7-O-glucoside (Yuanye Biotech, ≥ 98%), kaempferol 3-O-glucoside (Yuanye Biotech, ≥ 98%) or phlorizin (Yuanye Biotech, ≥ 98%). Each phenolic glycoside was dissolved in diet solution containing 30% sucrose and 5% yeast extract (weight/volume) until the target concentration of 10 μM was attained. The feeding chamber consisted of a vertically oriented glass tube (2 cm in diameter × 5 cm long), a black cotton plug and a tube sleeve. The top of the glass tube was sealed with one layer of Parafilm (Alcan Packaging) that was stretched as thinly as possible, and 0.2 mL of a diet solution was added to the outer surface of the Parafilm; the diet solution was then covered with another layer of Parafilm, such that the solution was sandwiched between the two layers of Parafilm at the top of the tube. Approximately 60 *B. tabaci* MED adults (mixed sexes) were then placed in the tube. Next, a black cotton plug was placed in the open end of the glass tube and the tube was covered with a tube sleeve. Tubes with diet solution without phenolic glycoside were used as controls. Each of the 11 treatments (11 phenolic glycosides) and the control was represented by three replicate tubes. The tubes were placed in an incubator at 25°C and 80% RH with a L14:D10 photoperiod. Mortality of *B. tabaci* adults was assessed after 96 h. Three independent biological replicates were performed for each treatment.

dsRNA synthesis and RNAi assays

To confirm the role of *BtPMaT1* in the detoxification of phenolic glycosides, the expression of *BtPMaT1* was knocked down by oral delivery of dsRNA to *B. tabaci* MED adults. Specific dsRNA primers of *BtPMaT1* and EGFP (GenBank accession no: KC896843) containing a T7 promoter on the 5′ end were designed (Table S1) using the SnapDragon tool (https://www.flyrnai.org/cgi-bin/RNAi_find_primers.pl) to avoid potential off-target effects. Furthermore, no specific hits with *BtPMaT2*, other insect or plant genes were detected by a BLASTn search against the NCBI non-redundant database, using the designed dsRNA fragment as query. An alignment of the *BtPMaT1* dsRNA fragment with its corresponding region in *BtPMaT2* or with XM_026027746.1, the closest homolog of *BtPMaT1* in tomato, also showed low nucleotide identity (45.02% and 43.54%, respectively) and only contained identical nucleotide stretches of maximum 5 to 7 bp. dsRNAs were then *in vitro* synthesized with the T7 Ribomax Express RNAi System (Promega).

RNAi was performed with the above described whitefly feeding setup (Figure 3A), using a diet solution containing dsRNA added between the two layers of Parafilm (200 μL of diet solution with 0.5 μg/μl dsRNA). RNAi efficacy was assessed by qPCR after the *B. tabaci* adults had fed for 48 h. The adults that had fed for 48 h on diet with dsRNA were then fed a solution containing phenolic glycosides or not for 96 h, and the survival was assessed. Each combination of dsRNA treatment and phenolic glycoside (including the diet solution with dsEGFP as control) was represented by three biological replicates.

VIGS assays

To determine the effect of continuous interference with the *BtPMaT1* gene on *B. tabaci* reproduction and performance, virus-induced gene silencing (VIGS) assays were carried out, and oviposition and whitefly survival were assessed. Virus vectors for VIGS (pTRV1 and pTRV2) (Figure 3I) have previously been described (Liu et al., 2002). The experimental protocol is shown in Figure 3J. A 456-bp fragment of the *BtPMaT1* gene was cloned from *B. tabaci* MED using specific primers (Table S1), and the PCR product was then cloned into *Xba*I-*Sac*I-cut pTRV2 to construct pTRV2-BtPMaT1. A 435-bp fragment of *EGFP* gene was cloned using specific primers (Table S1), and the PCR product was then cloned into *Xba*I-*Sac*I-cut pTRV2 to construct pTRV2-EGFP. The pTRV1, pTRV2-BtPMaT1 and pTRV2-EGFP vectors were transferred into *A. tumefaciens* GV3101 by electroporation, and the bacteria were selected on LB agar plates containing 100 μg/ml of rifampicin and 50 μg/ml of kanamycin. The *A. tumefaciens* harboring pTRV1, pTRV2-BtPMaT1 and pTRV2-EGFP were validated by PCR amplification. The *A. tumefaciens* containing pTRV1 and pTRV2 carrying the target gene were added to 5 mL of liquid LB medium containing 100 μg/ml of rifampicin and 50 μg/ml of kanamycin; the cultures were kept for 18 h at 30°C while shaking them at 200 rpm. A 2 mL volume of each culture was then added to 48 mL of liquid LB medium containing antibiotics as above with 200 μM acetosyringone; the cultures were once again kept for 18 h at 30°C while shaking at 200 rpm. The cultures were then centrifuged at 3000 × *g* for 10 min, and the pellets containing *A. tumefaciens* were resuspended in 5 mL of infiltration medium (200 μM acetosyringone, 10 mM MES, and 10 mM $MgCl_2$). The suspension was centrifuged again at 3000 × *g* for 10 min, and the pellets containing *A. tumefaciens* were resuspended in infiltration medium to obtain a final OD_{600} of 0.4. *A. tumefaciens* containing pTRV1 and pTRV2 with the target gene were mixed at a ratio 1:1. The mixture were infiltrated into the two largest true leaves of tomato plants (*Solanum lycopersicum* Miller, cv. Zhongza 9) using a 1 mL needleless syringe, tomato plants were left covered overnight. The infiltrated tomato plants were kept in a growth chamber at 27 ± 1°C, 70 ± 10% RH, and a photoperiod of L16:D8. After 20 days, RNA was extracted from the leaves of tomato plants and the cDNA was synthesized. With VIGS-specific primers (Table S1) and a tomato cDNA template, PCR was used to determine whether the VIGS vectors successfully

infected the tomato host. The successfully infected tomato plants (PMAT-VIGS tomato and EGFP-VIGS tomato) were used for further study.

To assess the effect of VIGS on whitefly performance, a clip cage (3.0 cm diameter and 2.5 cm height) was placed on one leaf of 12 successfully infected PMAT-VIGS tomato plants, and 10 newly emerged (< 24 h) female adults of *B. tabaci* MED were placed in each cage. Seven days later, the number of living adults and eggs laid on the leaf within the clip cages were counted to assess whitefly performance. Considering that *B. tabaci* is habitually parthenogenetic, and to exclude the effect of mating on the experiment, only female adults were used in this experiment. In an additional bioassay, 20 newly emerged (< 24 h) adults of *B. tabaci* MED (with the equal proportion of males and females) were added and after 7 days, the *B. tabaci* mortality in each clip cage was assessed. In all the assays, twelve EGFP-VIGS tomato plants were used as control.

Heterologous expression and protein purification

Recombinant BtPMaT1 was expressed in *Spodoptera frugiperda* Sf9 cells (Invitrogen) using the Bac-to-Bac Baculovirus Expression System (Invitrogen). The CDS of *BtPMaT1* gene (GenBank accession number MN756010) was subjected to codon optimization and synthesized with a C-terminal 6 × His tag sequence (TsingKe Biotech), and the obtained sequence was further validated with specific primers (Table S1). After validation, it was then cloned into the pFastBac1 vector (Invitrogen) to generate the pFastBac1-BtPMaT1 plasmid with BamHI and HindIII. Recombinant pFastBac1-BtPMaT1 plasmids were transfected to *E. coli* DH10Bac competent cells (Invitrogen), and the positive recombinant plasmids were then transfected to Sf9 cells using the Cellfectin II Reagent (Invitrogen). The Sf9 cells (1.0×10^6 cells/ml) were cultured in Sf-900 II SFM (Thermo Fisher Scientific) at 27 °C until the viral infection was clear, then P1 viral stock was harvested from the cell culture medium by centrifugation at 500 × *g* for 5 min and stored at 4°C in the dark. Recombinant protein in the pellets was determined by western blots using an Anti-His (C-term)-HRP Antibody and the SuperSignal West Pico Chemiluminescent Substrate (both Thermo Fisher Scientific). To obtain a suitable titer viral stock, the original P1 viral stock with multiplicity of infection (MOI) of 0.08 was transfected to Sf9 cells to generate a P2 stock. The recombinant protein was then expressed in Sf9 cells by transfection with the P2 titer stock. Three days after infection, cells were harvested and washed three times with PBS buffer (pH 7.4), then resuspended in Buffer A containing 1 mM PMSF and lysed by sonication. After centrifugation at 8000 × *g* at 4°C for 10 min, the recombinant protein in supernatants was purified by affinity chromatography using a His-Trap HP column (GE Healthcare). The sample was loaded with Buffer A (50 mM Tris–HCl, 200 mM NaCl, pH 8.3) and then eluted with buffer A with an imidazole gradient range from 50 to 250 nM. Protein eluates were added to a HiTrap desalting column (GE Healthcare) with Buffer B (50 mM Tris–HCl, pH 8.3) to remove imidazole, and were then subjected to ultrafiltration with Buffer C (50 mM potassium phosphate, 5 mM 2-mercaptoethanol, pH 8.0) in a 30-kDa cutoff Amicon Ultra-0.5 Device (Millipore).

Metabolic experiments

In an initial BtPMaT1 activity survey, the reaction mixture consisting of Sf9-expressed (10 μg) purified BtPMaT1 protein, 0.2 mM of a phenolic glycosides, and 0.2 mM malonyl-CoA (Sigma-Aldrich, ≥ 90%) in 450 μL of Buffer C. The mixture was made separately for each of the 11 tested phenolic glycosides (see Phenolic glycoside assays) and three additional flavonoid glycosides [quercetin 3-O-β-D-glucoside/isoquercetrin (Meilunbio, ≥ 98%), apigenin-7-O-glucoside/apigetrin (Psaitong, ≥ 98%) and naringenin-7-O-glucoside/prunin (Psaitong, ≥ 98%)]. The reaction mixture without the BtPMaT1 protein was used as the control. The reactions were incubated at 30°C for 1 h and were stopped by adding 450 μL of methanol (HPLC grade, Thermo Fisher Scientific). After centrifugation at 12000 × *g* at 4°C for 20 min, the reaction supernatants were analyzed using the ACQUITY UPLC I-Class/Xevo G2-XS QTOF system (Waters) equipped with an ACQUITY UPLC BEH C18 column (2.1 mm × 50 mm, 1.7 μm particle size). The column temperature and sample temperature were 30°C and 20°C, respectively. An acetonitrile/water (0.1% formic acid) gradient elution was carried out at a flow rate of 0.2 ml/min as follows: 0-3 min (2%–15% acetonitrile), 3-6 min (15%–40% acetonitrile), 6-9 min (40%–60% acetonitrile), and 9-20 min (60%–98% acetonitrile), with an injection volume of 10 μl. Mass spectrometry (MS) was conducted in the range of 50-900 Da (full-scan MS) in negative ion mode, and the data were analyzed with the Progenesis QI/EZ Info software (Waters).

For the determination of the enzymatic activity of the Sf9-expressed recombinant BtPMaT1 protein, 0.1 mM of a phenolic glycoside (either kaempferol 3-O-glucoside, kaempferol 7-O-glucoside, rhaponticin, isoquercetrin, apigetrin or prunin) and 0.2 mM malonyl-CoA were added to the reaction mixture with 5 μg of purified BtPMaT1 protein. The mixture was incubated at 30°C for 30 min, each reaction was replicated twelve times. For the determination of the enzymatic activity of the extracted whitefly gut proteins, 0.01 mM of a phenolic glycoside (either kaempferol 3-O-glucoside, kaempferol 7-O-glucoside, rhaponticin, isoquercetrin, apigetrin or prunin) and 0.2 mM malonyl-CoA were added to the reaction mixture with 50 μg of whitefly gut proteins. The mixture was incubated at 30°C for 1 h, each reaction was replicated five times. The enzymatic activity was measured by MS as described above, with peonidin-3-glucoside (Sigma-Aldrich, ≥ 97%) as an internal standard. One enzymatic unit was defined as nmol product increment per mg of BtPMaT1 protein per min at 30°C.

To determine whether BtPMaT1 can detoxify phenolic glycosides, the mortality of *B. tabaci* adults was measured after they had fed on a diet solution without phenolic glycoside (control), a solution with a representative phenolic glycoside (kaempferol 3-O-glucoside) (Yuanye Biotech, ≥ 98%) or with its corresponding phenolic malonylglucoside [kaempferol 3-O-(6-malonyl-glucoside)] (BOC Sciences, ≥ 95%) for 96 h. The experimental procedure and treatment concentrations were the same as the aforementioned phenolic glycoside bioassays. Three independent biological replicates were performed for each treatment.

Honeydew analysis

To further determine whether BtPMaT1 is responsible for the malonylation of phenolic glucosides in *B. tabaci*, we performed RNAi, and then honeydew was collected and analyzed by UPLC-QTOF/MS after feeding whiteflies with kaempferol 3-O-glucoside. Kaempferol 3-O-glucoside was dissolved in diet solution (described above) with the final concentration of 10 μM. The honeydew collection device consists of a vertically oriented plastic tube (6 cm in diameter × 1 cm long), and a plastic bottom covered with tinfoil. Two hundred newly emerged whitefly adults fed dsRNA for 48 h on diet solution were transferred into the honeydew collection device, and honeydew was then collected and weighed after adults fed on the phenolic glycoside solution for 48 h. The obtained honeydew was dissolved in deionized water to the final concentration of 0.1 g/ml and isochoric methanol was added. Kaempferol 3-O-glucoside and its malonylation product were analyzed using QTOF/MS and quantified based on their precursor molecular ions in negative ion mode, *m/z* 447.0780 for kaempferol 3-O-glucoside and *m/z* 533.0801 for kaempferol 3-O-malonylglucoside, respectively. Each RNAi treatment (dsEGFP or dsBtPMaT1) was biologically replicated three times.

Similarly, honeydew of *B. tabaci* fed on wild-type and transformed tomato plants (see "Transgenic experiments" section) were collected by transferring newly emerged *B. tabaci* adults into a clip cage (with tinfoil on the bottom), which was placed on one leaf of tomato plants for 48 h. The honeydew was dissolved with deionized water to the final concentration of 0.1 g/ml then isochoric methanol was added. Whole-scale analysis of phenolic glucosides in honeydew was performed using the same method as for detection of BtPMaT1 activity (UPLC-QTOF-MS; Waters ACQUITY UPLC I-Class/Xevo G2-XS QTOF), and the scan was in the range of 50-1200 Da with full-scan in negative ion mode. The Natural Products Application Library integrated in the UNIFI Scientific Information System (Waters) was used to analyze the MS data to identify potential flavonoids. The flavonoid glucosides and malonylated flavonoid glucosides were manually filtered from the identified compounds. The honeydew experiments were conducted for three biological replicates. Raw data were processed using Progenesis QI for peak picking and alignment, one-way ANOVA with Holm-Sidak's tests and Variable Importance for the Projection (VIP) plot analysis were used to determine significant differences in phenolic glucosides levels (Figure 5; Table S3), with detailed mass features being shown in Table S4.

Transgenic experiments

Transgenic tomato lines were developed by introducing the hairpin RNA expression vector [pCAMBIA-RNAi-*BtPMaT1*, containing a cauliflower mosaic virus 35S promoter, driving expression in many plant tissues including the phloem (Nilsson et al., 1996)] into tomato (*Solanum lycopersicum* cv. Moneymaker). The construction of hairpin RNA expression vector (Figure S7A) has been described previously (Xiong et al., 2013). A 444-bp target fragment of *BtPMaT1* was cloned from *B. tabaci* MED using Sense-BtPMaT1 primers (Table S1), and the PCR product was then cloned into *Xho*I-BglII-cut pRNAi1017 (pRNAi-Sense-*BtPMaT1*). The anti-sense fragment of *BtPMaT1* was cloned from *B. tabaci* MED using Anti-sense-BtPMaT1 primers (Table S1), the purified product was then cloned into *Bam*HI-*Sal*I-cut pRNAi-Sense-*BtPMaT1* (pRNAi-*BtPMaT1*). The pRNAi-*BtPMaT1* vector was digested with *Pst*I and cloned into *Pst*I-cut pCAMBIA2300-35S-OCS (pCAMBIA-RNAi-*BtPMaT1*). *A. tumefaciens* LBA4404 based transformation was used to transfer the recombinant pCAMBIA-RNAi-*BtPMaT1* plasmid into tomato as described previously (Park et al., 2003). To verify the success of the transformation, gDNA of putative transgenic and non-transgenic tomato leaf was extracted using the Plant Genomic DNA Kit (TIANGEN), and the extracted DNA was subjected to PCR using detection primers (Table S1). Northern blot analyses were performed to test whether dsRNAs was stably expressed in transgenic tomato lines. Total RNA samples were extracted from transgenic or non-transgenic tomato leaves using TRIzol reagent (Invitrogen). Total RNAs (10 μg per lane) were electrophoretically separated by 1.0% formaldehyde-containing agarose gels, then transferred onto a Hybond-N^+ nylon membranes (GE Healthcare). For siRNA analysis, cellular RNA samples (approximately 20 μg per lane) were separated by 15% polyacrylamide gels with 7 M urea and 0.3 M sodium acetate. The separated RNA samples were transferred onto Hybond nylon membranes using Trans-Blot SD. Semi-Dry Transfer Cell (Bio-Rad) according to manufacturer's instructions, subsequently, cross-linking of RNA was achieved by exposure to UV light. Specific DNA probes were obtained from the PCR products (generated by gene-specific primers) labeled with DIG-UTP (Roche). qPCR analyses were carried out to assess the RNAi efficacy on *B. tabaci* MED adults feeding on transgenic tomato lines, *B. tabaci* adults feeding on non-transgenic tomato lines were used as control. RNAi efficacy was determined every two days for seven days.

To investigate whitefly performance on the transgenic tomato lines, 20 whitefly adults (with an equal proportion of males and females) were released into clip cages attached to one transgenic tomato plant leaf (as described above). Whitefly mortality was assessed every two days for seven days. Six transgenic and six control plants were used for this study, with 2 clip cages per seedling for a total of 12 per treatment. In addition, a simulated field assay was conducted to further evaluate how whiteflies performed on the transgenic tomato lines. Whitefly adults were collected and transferred to transgenic tomato plants (approximately 500 whiteflies per tomato plant) in a cage (60 cm length, 40 cm width and 80 cm height), mortality was assessed after 7 days of feeding. Five transgenic and five control plants were used for this study.

To determine whether the transgenic tomato plants had no undesirable effects on non-target arthropods, 10 fourth-instar nymphs of the aphid *M. persicae* were placed into a clip cages attached to a tomato leaf. After seven days, the number rather than the mortality of *M. persicae* in each clip cage was recorded for bioassays owing to the reproductive characteristics including parthenogenesis and ovoviviparity of *M. persicae*. Six transgenic and six control plants were used in this study, with 2 clip cages per plant and, hence, 12 clip cages per treatment. For simulated field assay, fourth-instar *M. persicae* were carefully transferred onto tomato plants (150 aphids per tomato plant) in a cage, as described above for the whiteflies. Aphid numbers were recorded after 7 days of feeding. Five transgenic and five control tomato plants were used for this assay.

In a separate series of experiments, transgenic and non-transgenic tomato plants were also challenged with the spider mite *T. urticae*. Adult female mites were transferred to fresh transgenic tomato leaves (20 *T. urticae* mites per leaf) with wet cotton strips wrapped around the petioles. Then, the tomato leaves were placed on moist sponges in Petri dishes, surrounded by cotton strips to prevent *T. urticae* from escaping. Every two days, the surviving mites were carefully transferred onto a new tomato leaf of the same type and were maintained under the same conditions. The mortality of spider mites was calculated after seven days. For a simulated field assay, adult spider mite females were carefully transferred onto tomato plants (with approximately 200 *T. urticae* mites per tomato plant) in a cage, mortality was assessed after 7 days of feeding on the plants. In each case five transgenic and five non-transgenic tomato plants were used.

QUANTIFICATION AND STATISTICAL ANALYSIS

All the data were analyzed using IBM SPSS Statistics (ver. 23.0) software (IBM Corp.). Data are shown as the means ± SEM. Determination of statistical significance was achieved using one-way ANOVA with Holm-Sidak's tests (*, $p < 0.05$; **, $p < 0.01$; ***, $p < 0.001$).

Supplemental figures

A

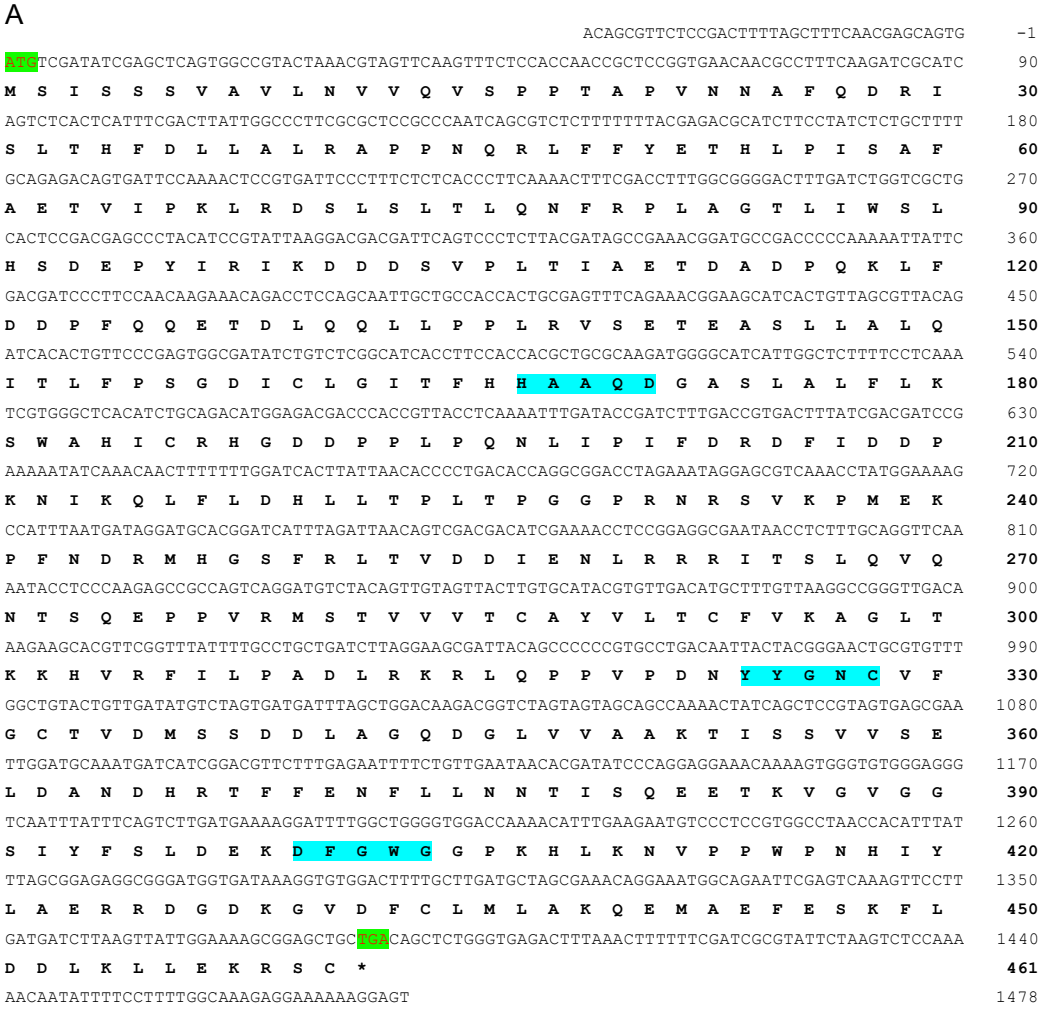

B

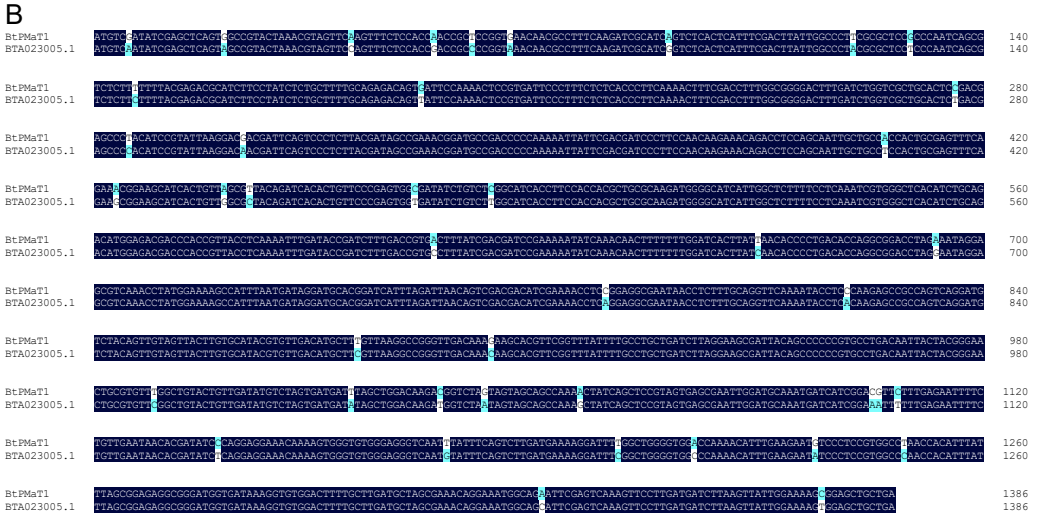

(legend on next page)

Figure S1. Sequence analysis of the *BtPMaT1* gene, related to Figure 1

(A) Nucleotide and deduced amino acid sequence of the *BtPMaT1* gene. The nucleotide and amino acid position of the *BtPMaT1* gene are shown on the right. The start codon (ATG) and stop codon (TAG) are in red and highlighted in green. Two highly conserved domains of plant BAHD acyltransferases, the catalytic HXXXD and the structural DFGWG motifs, and the typical YXGNC motif for phenolic glycoside and anthocyanin malonyltransferases, are highlighted in light-blue. (B) Sequence comparison between the PCR-cloned and the genome-predicted CDS sequences of *BtPMaT1* gene.

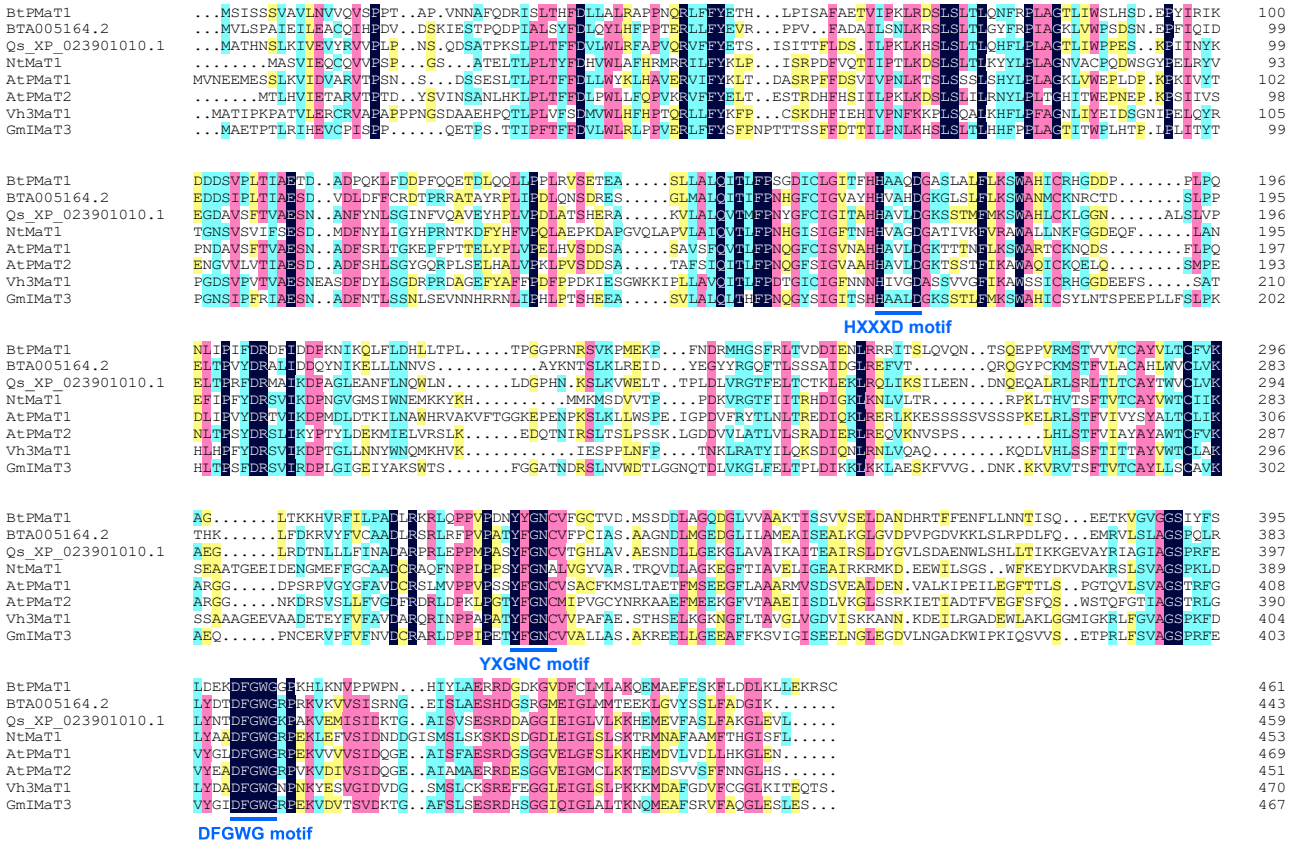

Figure S2. Amino acid sequence alignment of BtPMaT1 and its homologs in different plant species, related to Figure 1

Plant homologs of BtPMaT1 were retrieved from the GenBank or TAIR database. Gene names and or accessions are indicated on the left, and the highly conserved HXXXD, DFGWG and YXGNC motifs are denoted. Abbreviation: BtPMaT1 (*B. tabaci*, MN756010); BTA005164.2 (*B. tabaci*); Qs_XP_023901010.1 (*Quercus suber*); NtMaT1 (*Nicotiana tabacum*, NP_001312260.1); AtPMaT1 (*Arabidopsis thaliana*, AT5G39050.1); AtPMaT2 (*A. thaliana*, AT3G29670.1); Vh3MaT1 (*Verbena hybrida*, AAS77403.1); GmIMaT3 (*Glycine max*, NP_001237760.1).

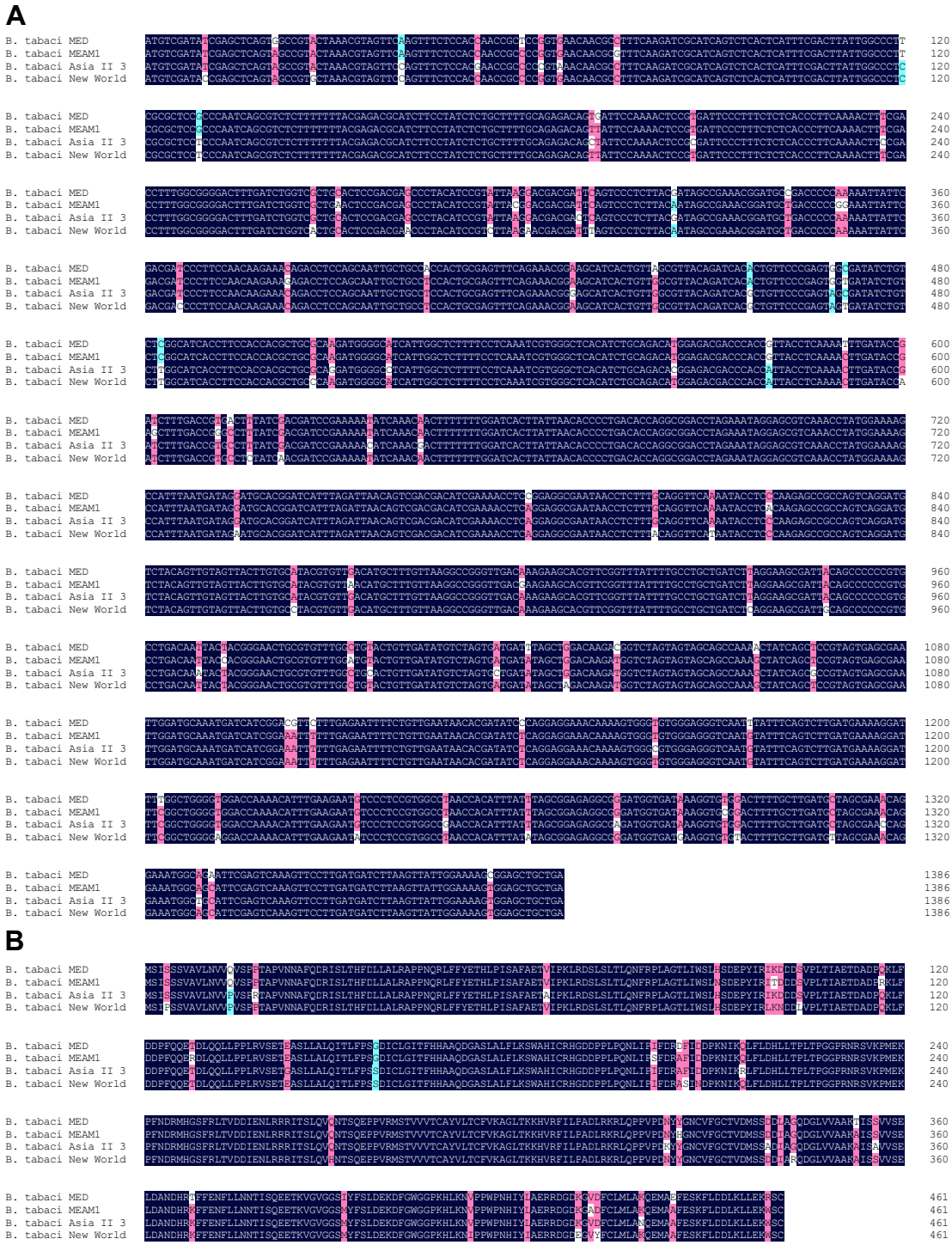

Figure S3. Nucleotide and amino acid sequence comparison of *BtPMaT1* in different cryptic species of *B. tabaci*, related to Figure 1

(A) Nucleic acid sequence alignment of *BtPMaT1*. The species names are indicated on the left. (B) Amino acid sequence alignment of *BtPMaT1*. The species names are indicated on the left. Sequences were derived from the GenBank database (*B. tabaci* MEAM1 (GenBank accession number XM_019041511) or have been deposited in the GenBank database: *B. tabaci* MED (GenBank accession number MN756010), *B. tabaci* Asia II 3 (GenBank accession number MW387251) and *B. tabaci* New World (GenBank accession number MW387250).

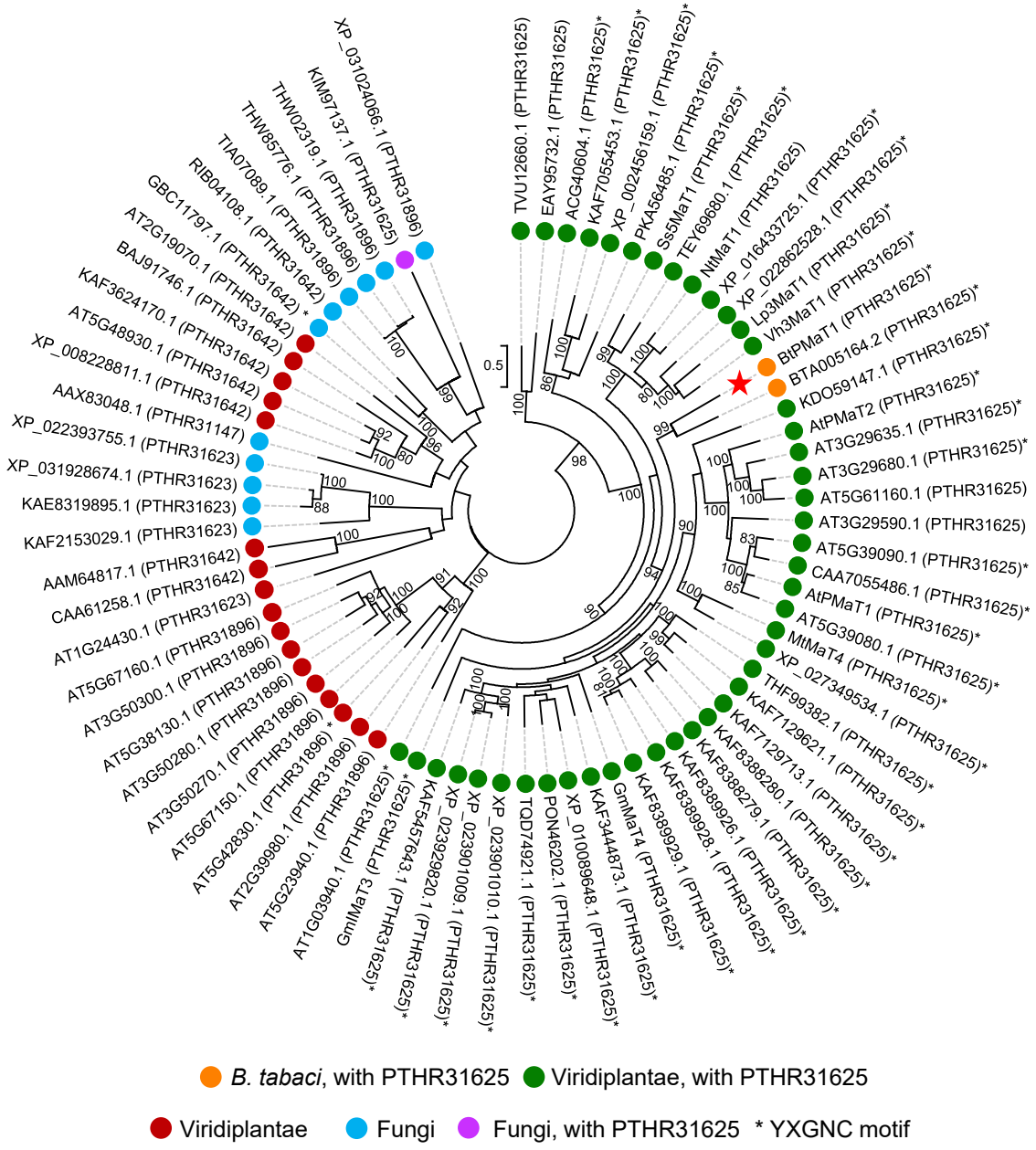

Figure S4. Maximum likelihood phylogenetic analysis of BtPMaT1 and BtPMaT2, related to Figure 1

Sequences corresponding to accession numbers or enzyme names in the tree can be extracted from the GenBank database, TAIR (Berardini et al., 2015) or from previous studies (Bontpart et al., 2015; Tuominen et al., 2011; Yu et al., 2009). PANTHER domains present in protein sequences are shown between brackets. Only bootstrap values above 80 are shown. An asterisk indicates the presence of the YXGNC motif, typical for phenolic glycoside and anthocyanin malonyltransferases (D'Auria, 2006; Tuominen et al., 2011; Zhao et al., 2011). The tree is midpoint rooted and the scale bar represents 0.5 amino acid substitutions per site. The sequence alignment used for phylogenetic analysis can be found in the Data S1.

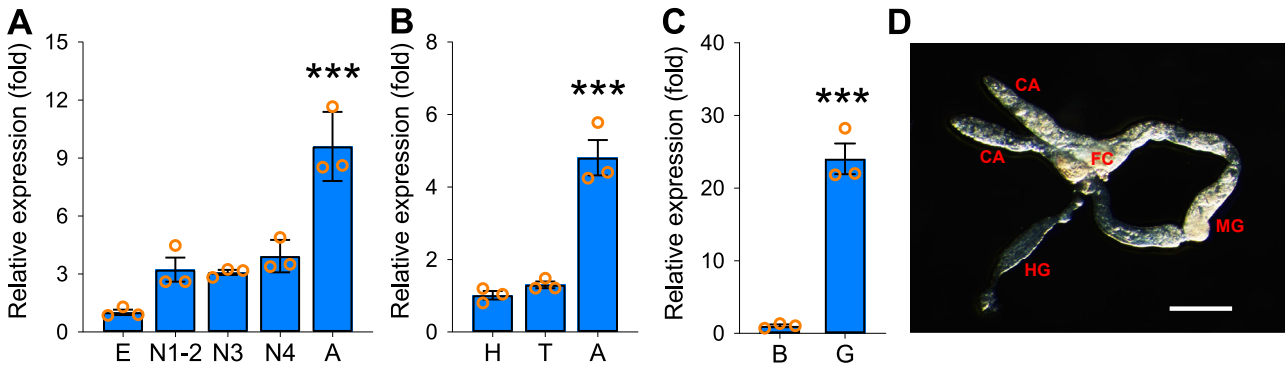

Figure S5. The spatio-temporal expression pattern of *BtPMaT1* in different developmental stages and parts of the body of *B. tabaci* MED, related to STAR methods

(A) Relative expression levels of *BtPMaT1* in eggs (E), 1st- and 2nd-instar nymphs (N1-2), 3rd-instar nymphs (N3), 4th-instar nymphs (N4) and adults (A) were determined by qPCR. (B, C) Relative expression levels of *BtPMaT1* in adult head (H), thorax (T), abdomen (A), non-gut body (B) and gut (G) were determined by qPCR. Both of the *EF1-α* and *RPL29* genes were used as internal reference genes. Values are means ± SEM, n = 3 biologically independent samples, ***$p < 0.001$ one-way ANOVA with Holm-Sidak's test was used for comparison. (D) The structure of the dissected gut tissues from *B. tabaci* MED adults. Abbreviations: MG, midgut; FC, filter chamber; CA, cecae; HG, hindgut. The scale bar is 100 μm.

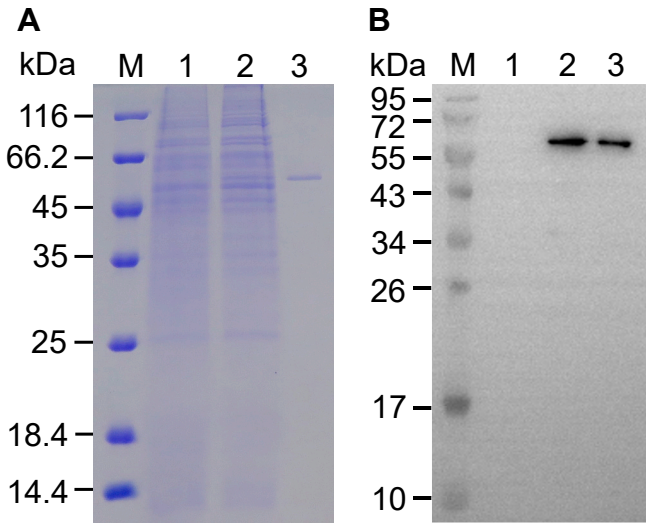

Figure S6. Heterologous expression of the recombinant BtPMaT1 protein in Sf9 cells and detected by western blots, related to Figure 4

(A) The expression and purification of BtPMaT1 protein in Sf9 cells detected by SDS-PAGE. (B) Protein detection by western blots. Lane M, protein marker; lane 1, supernatant of ultrasonically disrupted Sf9 (control) cells; lane 2, supernatant of ultrasonically disrupted Sf9 (BtPMaT1) cells; lane 3, purified BtPMaT1 protein.

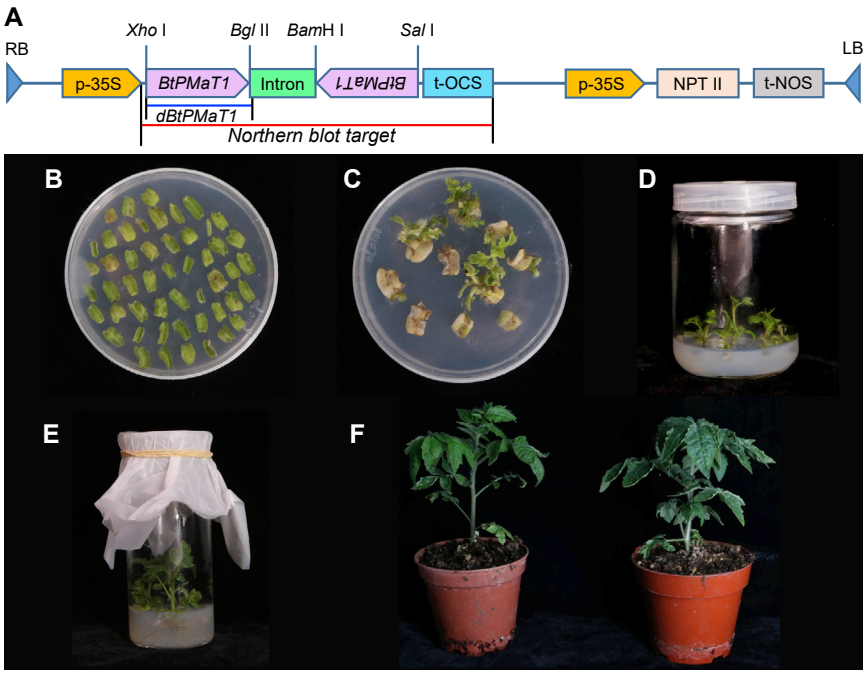

Figure S7. The dsRNA-expressing vector, genetic transformation, and regeneration of transgenic tomato lines, related to Figure 6

(A) The schematic representation of the pCAMBIA-RNAi-*BtPMaT1* expression cassette used for tomato transformation. The target segment for transgenic detection is highlighted in blue, and the target segment for northern blot is highlighted in red. (B and C) The calli were induced on the synthetic medium containing kanamycin. (D) Somatic embryogenesis of transgenic tomato lines. (E) Plant regeneration of tomato lines. (F) Regenerated tomato lines cultured in soil.